







## Article

# Extraction of Bioactive Compound-Rich Essential Oil from *Cistus ladanifer* L. by Microwave-Assisted Hydrodistillation: GC-MS Characterization, In Vitro Pharmacological Activities, and Molecular Docking

Naoufal El Hachlafi <sup>1,\*</sup>, Fahd Kandsi <sup>2</sup>, Amine Elbouzidi <sup>3</sup>, Fatima Zahra Lafdil <sup>2</sup>, Ghizlane Nouioura <sup>4</sup>, Emad M. Abdallah <sup>5</sup>, Rhizlan Abdnim <sup>2</sup>, Mohamed Bnouham <sup>2</sup>, Samiah Hamad Al-Mijalli <sup>6</sup>, Hanae Naceiri Mrabti <sup>7,8</sup> and Kawtar Fikri-Benbrahim <sup>9</sup>

- <sup>1</sup> Laboratory of Pharmacology and Toxicology, Bio Pharmaceutical and Toxicological Analysis Research Team, Faculty of Medicine and Pharmacy, University Mohammed V in Rabat, Rabat 6203, Morocco
  - <sup>2</sup> Laboratory of Bioresources, Biotechnology, Ethnopharmacology and Health, Faculty of Sciences, Mohammed First University, Oujda 60000, Morocco
  - <sup>3</sup> Laboratoire D'Amélioration des Productions Agricoles, Biotechnologie et Environnement (LAPABE), Faculté des Sciences, Université Mohammed Premier, Oujda 60000, Morocco
  - <sup>4</sup> Laboratories of Natural Substances, Pharmacology, Environment, Modeling, Health and Quality of Life (SNAMOPEQ), Faculty of Sciences, Sidi Mohamed Ben Abdellah University, Fez 30000, Morocco
  - <sup>5</sup> Department of Science Laboratories, College of Science and Arts, Qassim University, Ar Rass 51921, Saudi Arabia
  - <sup>6</sup> Department of Biology, College of Sciences, Princess Nourah bint Abdulrahman University, P.O. Box 84428, Riyadh 11671, Saudi Arabia
  - <sup>7</sup> High Institute of Nursing Professions and Health Techniques Casablanca, Casablanca 20250, Morocco
  - <sup>8</sup> Euromed Research Center, Euromed Faculty of Pharmacy, School of Engineering and Biotechnology, Euromed University of Fes (UEMF), Meknes Road, Fez 30000, Morocco
  - <sup>9</sup> Laboratory of Microbial Biotechnology and Bioactive Molecules, Sciences and Technologies Faculty, Sidi Mohamed Ben Abdellah University, Imouzzzer Road, Fez 30000, Morocco
- \* Correspondence: naoufal.elhachlafi@usmba.ac.ma



**Citation:** El Hachlafi, N.; Kandsi, F.; Elbouzidi, A.; Lafdil, F.Z.; Nouioura, G.; Abdallah, E.M.; Abdnim, R.; Bnouham, M.; Al-Mijalli, S.H.; Naceiri Mrabti, H.; et al. Extraction of Bioactive Compound-Rich Essential Oil from *Cistus ladanifer* L. by Microwave-Assisted Hydrodistillation: GC-MS Characterization, In Vitro Pharmacological Activities, and Molecular Docking. *Separations* **2024**, *11*, 199. <https://doi.org/10.3390/separations11070199>

Academic Editor: Antonio Canals

Received: 8 June 2024

Revised: 21 June 2024

Accepted: 24 June 2024

Published: 27 June 2024



**Copyright:** © 2024 by the authors. Licensee MDPI, Basel, Switzerland. This article is an open access article distributed under the terms and conditions of the Creative Commons Attribution (CC BY) license (<https://creativecommons.org/licenses/by/4.0/>).

**Abstract:** *Cistus ladanifer* L. is an aromatic and resinous perennial shrub commonly used in Moroccan folk medicine against a range of illnesses including skin problems, diabetes, diarrhea, and inflammation. The current investigation aims to determine the bioactive compounds of *C. ladanifer* essential oil (CL-Eo) extracted by microwave-assisted hydrodistillation and their biological properties using in vitro and molecular docking approaches. The GC-MS analysis identified linderol (17.76%), gamma-terpinene (17.55%), and borneol (13.78%) as main bioactive compounds. CL-Eo significantly inhibited  $\alpha$ -amylase ( $IC_{50} = 0.41 \pm 0.009$  mg/mL),  $\alpha$ -glucosidase ( $IC_{50} = 0.49 \pm 0.002$  mg/mL) and lipase ( $IC_{50} = 0.45 \pm 0.004$  mg/mL) enzymes. Moreover, CL-Eo showed significant hemoglobin glycation as well as antioxidant capacity as indicated by DPPH, ABTS, Frap and beta-carotene tests. The antimicrobial evaluation used disc-diffusion and microdilution tests in vitro. The results showed that CL-Eo had significant antibacterial activity, particularly against *P. mirabilis* ( $17.16 \pm 1.04$  mm), and moderate effects against *L. innocua* ( $13.48 \pm 1.65$  mm) and *E. coli* ( $12.47 \pm 0.61$  mm). In addition, it demonstrated potent antifungal activity against *C. albicans* ( $18.01 \pm 0.91$  mm) and *C. tropicalis* ( $16.45 \pm 0.32$  mm). The MIC and MBC tests provided confirmation that CL-Eo exhibited potent growth inhibition. The MIC ranged from 0.25 to 8.0% v/v and the MBC or MFC ranged from 0.25 to 16.0% v/v Eo. The tolerance level ratio showed bactericidal and fungicidal effects against tested microbial strains in varying degrees. According to these data, CL-Eo might be suggested as a promising candidate for drug development, specifically for combating candidiasis and diabetes.

**Keywords:** volatile compounds; phytochemicals; biological properties; enzyme inhibitors; diabetes; anti-bacterial agents; computational analysis

## 1. Introduction

The environment consists exclusively of organic natural products, which have served as the main source of vital supplies for human life since the beginning of civilization millennia ago [1]. Plants have been the main source of medicines and therapies throughout history and across diverse human cultures until the Industrial Revolution began in the eighteenth century. During the late 19th and early 20th centuries, there was a significant risk of the progressive eradication of herbal remedies from medical treatment, as they were being replaced by chemical and synthetic drugs [2,3]. In recent years, a resurgence of interest in the field of medicinal plants has been observed. Research efforts have been undertaken by professional scientists in fields such as alternative medicine, pharmacognosy, pharmacotherapy, microbiology, medicinal chemistry, botany, organic chemistry, biochemistry and molecular biology to uncover novel chemical constituents in medicinal plants [4–6]. Contemporary biotechnologies in synthetic chemistry, computational modeling, and chemical informatics are being utilized by the researchers [7–9].

Furthermore, diabetes mellitus is a chronic metabolic disorder characterized by hyperglycemia, affects millions worldwide and is accompanied by significant morbidity and mortality due to complications like cardiovascular disease, neuropathy, nephropathy, and retinopathy [10,11]. Oxidative stress is a crucial factor in both the development and progression of diabetes. It involves the alteration of several physiological functions, contributing to the pathophysiology of the diabetes via various mechanisms, including dysfunction of  $\beta$ -cell, insulin resistance, endothelial destruction, and activation of stress pathways such as Protein Kinase C (PKC) and Endoplasmic Reticulum (ER) stress [12–14]. Overall, conventional treatments often comprise lifestyle modifications, oral hypoglycemic agents, and insulin treatment. However, there is growing interest in complementary and alternative therapies, including the use of essential oils (Eos), for managing diabetes and its complications.

In fact, Eos are volatile aromatic components isolated from plants through different extraction methods. These oils capture the plant's scent and flavor and have been used for centuries in traditional medicine for their beneficial effect [5,15,16]. They possess a plethora of bioactive molecules, such as terpenes, aldehydes, ketones, and phenols, which contribute to their health benefits [17–20]. Several extraction techniques, including steam distillation, solvent extraction, and supercritical fluid extraction and microwave-assisted extraction (MHD) have been employed to isolate Eos [21]. In the case of *C. ladanifer* Eo, generally steam distillation is used for oil extraction [22,23]. However, conventional methods such as MHD have not yet been employed.

Indeed, MHD is a versatile method for extracting appreciated components from medicinal plants, adaptable for both small-scale and large-scale extractions. MHD is renowned for its excellent performance in terms of the quantity and quality of the extracted Eos, along with its time and cost efficiency. This method also significantly reduces energy usage and lowers carbon dioxide emissions, contributing to its widespread adoption in both laboratory and industrial contexts [24]. Key advantages of MHD include rapid energy transfer, effective heating, and an environmentally friendly isolation process [25].

*Cistus ladanifer* L. (*C. ladanifer*) is an aromatic and resinous perennial shrub that belongs to the Cistaceae family. It is prevalent in forest areas and uncultivated parts of the western Mediterranean region, including Portugal, Spain, southern France, and northern Morocco, compared to other wild species [26]. The predominant species include *C. ladanifer*, *C. laurifolius*, *C. salvifolius*, *C. monspeliensis*, *C. albidus* and *C. creticus*. There are two varieties of *C. ladanifer* in Morocco, distinguished mostly by the color of their flower petals. *C. ladanifer* var. *albiflorus* Dun has entirely white petals, while *C. ladanifer* var. *maculatus* Dun has petals that are marked with red spots [26]. *C. ladanifer* is used in Moroccan traditional medicine as a multipurpose treatment for a range of illnesses including skin problems, diabetes, diarrhea, and inflammation [27]. Moreover, *Cistus ladanifer* Eo (CL-Eo) have shown to possess promising antibacterial and antioxidant properties [22,23]. However, studies on

other pharmacological properties, such as the antidiabetic and anticandidal effects of this oil, are restricted.

In this context, the current exploration aims to investigate the volatile oil of Moroccan CL-Eo extracted by microwave-assisted hydrodistillation and to determine its multifaceted biological effects by adopting *in vitro* and molecular docking approaches. To the best of the authors' knowledge, there is no available study on the inhibition of glycation and lipase enzyme by CL-Eo. In addition, this investigation is also the first to report the molecular docking simulation to expect the feasible binding patterns and affinities of the detectable bioactive compounds of CL-Eo with specific targets. On the other hand, the existing knowledge of the antimicrobial and antioxidant properties of this plant needs additional elucidation. To this end, this work brings valuable evidence to this area.

## 2. Material and Methods

### 2.1. Plant Material

The aerial parts of *C. ladanifer* were gathered from the Aknoul region, Morocco (34°38'59" N, 3°52'00" W) in May 2023 at flowering time. The botanical validation was performed at the Department of Biology, Faculty of Sciences and Technologies, Fez, under identifier BLMUP 516.

### 2.2. Eo Extraction by Microwave-Assisted Hydrodistillation

Eo extraction was performed using a microwave oven as a power source. Precisely, the Whirlpool MWD 119 model from Germany, with a 20 L capacity and operating at a frequency of 2.45 GHz, was utilized. This microwave oven was directly joined with Clevenger-type device and equipped with a freezing system to guarantee constant condensation of the extract. The oven functioned at 1100 Watts, with a power supply of 230 V at 50 Hz and cavity dimensions of 260 × 442 × 355 mm. In brief, 150 g of the aerial part of *C. ladanifer* were mixed with 1.5 L of distilled water in a flask and heated in the microwave oven cavity at 600 W for 35 min. The vapor mixture of water and volatile oil was constantly compressed via an extraneous freezing system allied with a microwave cavity, and then the extract was gathered in a Clevenger receiver [24].

After the extraction, the volatile oil was recuperated and desiccated with anhydrous sodium sulfate.

The extraction yield is calculated by adopting the following formula:

$$\text{Yield(\%)} = \frac{\text{Moil}}{\text{Msample}}$$

where Moil is the mass of oil in grams, while Msample signifies the mass of the plant material in grams.

Finally, prior to experiments, the Eo was kept in adequate conditions (at 4 °C in the dark).

### 2.3. GC–MS Analysis

A chromatography system coupled with a mass spectrometer (GC-MS) (Kyoto, Japan) was utilized for the separation and identification of components, featuring a BPX25 capillary column containing a 95 percent dimethylpolysiloxane diphenyl phase. The QP2010 mass detector was incorporated into this process (Kyoto, Japan). Pure helium served as the carrier gas, delivered at a constant flow rate of 3 mL/min. The assessed mass range spanned from 40 to 300 *m/z*. In the analytical process, the oil produced was introduced into the chamber and blended with a suitable solvent. Following this, 1 µL of the prepared oil, diluted with the same suitable solvent, was injected in fractionation mode, with a 90:1 split ratio. Each sample underwent three independent assessments. Compound identification was conducted by likening retention times with certified standards and aligning mass spectrum fragmentation patterns with those available in catalogs or associated with NIST compounds, and all data were treated employing the Laboratory Solutions software (version 2.5).

#### 2.4. Molecular Docking Protocol

The molecular docking simulation was executed as outlined in references [28–30]. Protein structures can be found of tyrosinase, inflammation, and diabetes target proteins, tyrosinase (PDB ID: 5I3B) [31,32], lipoxygenase (LOX, PDB ID: 1N8Q) [29], and three diabetes-involved proteins  $\alpha$ -amylase (PDB ID: 1SMD) [33],  $\alpha$ -Glucosidase (PDB ID: 5NN5) [34], pancreatic lipase (PDB ID: 1LPB) [35]. The protein structures were provided by the Protein Data Bank (<https://www.rcsb.org/structure> retrieved on 9 January 2024), in a crystallographic 3D structure and utilized as docking targets, employing Autodock Tools (version 1.5.6). The protein structures were devoid of water molecules, metal atoms, co-crystallized ligands, and other non-covalently attached components. After incorporating Kollman charges, polar hydrogens, and merging nonpolar hydrogens, the target file was saved in the suitable pdbqt format. The ligands found in CL-Eo were synthesized in the following manner: An sdf (3D conformer) file was obtained from PubChem (<https://pubchem.ncbi.nlm.nih.gov/>) on 9 January 2024 and subsequently transformed into a pdb file using PyMol. The ligand's ultimate pdbqt file was acquired through the utilization of Autodock Tools (version 1.5.6). The Autodock Vina software's built-in scoring mechanism was used to perform rigid molecular docking [16]. The grid box demonstrating the docking search space was adjusted to optimize its alignment with the active binding site [32,36]. The data for the complexes of docked ligands were provided in the form of  $\Delta G$  binding energy values (kcal/mol). The software Discovery Studio 4.1, developed by Dassault Systems Biovia in San Diego, CA, USA, was utilized to analyze the interactions between proteins and ligands, as well as to create 2D representations of molecular interactions.

#### 2.5. Antidiabetic Activity

##### 2.5.1. $\alpha$ -Amylase Inhibition Assay

The evaluation of  $\alpha$ -amylase inhibition was carried out based on the procedure outlined by [37], with minor adjustments made for this study. A mixture comprising 100  $\mu$ L of 0.2 M phosphate buffer (pH 6.9) and 100  $\mu$ L of  $\alpha$ -amylase enzymatic solution (13 IU) was combined with 100  $\mu$ L of either CL-Eo or acarbose at various concentrations (0.065, 0.125, 0.25, 0.5, and 1 mg/mL). Afterward, this mixture was preincubated at 37 °C for 10 min. Following the preincubation, 100  $\mu$ L of a 1% starch solution was introduced into the reagent mixture. The resulting blend underwent a second incubation at 37 °C for 20 min. To halt the reaction at the end of the incubation period, a colored reagent known as 3,5-dinitrosalicylic acid was added. The reaction mixture was then subjected to an additional incubation in a 100 °C water bath for 8 min to develop color intensity. Subsequently, the samples were chilled in an ice-cold water bath for 5 min. After dilution with 1 mL of distilled water, the inhibitory action on  $\alpha$ -amylase was determined using a spectrophotometer at 540 nm.

##### 2.5.2. $\alpha$ -Glucosidase Inhibition Test

A solution of alpha-glucosidase (0.1 U/mL) was prepared in a 100 mM phosphate buffer (pH 7.5), and the substrate used was 0.1 mL of sucrose (50 mM). To this solution, 20  $\mu$ L of CL-Eo at various concentrations was added, and the mixture was incubated at 37 °C for 20 min. The reaction was ended by heating it to 100 °C for 5 min. Subsequently, the absorbance was measured at 500 nm using a spectrophotometer, as outlined by [38]. The concentration of glucose released during the reaction was determined using a commercial kit based on the glucose oxidase method.

##### 2.5.3. Pancreatic Lipase Inhibition Test

The lipase inhibition assay was performed as previously reported by McDougall et al. [39]. Various dilutions of CL-Eo were prepared at distinct concentrations. For the inhibition activity test, 100  $\mu$ L of lipase, 200  $\mu$ L of CL-Eo, and 700  $\mu$ L of Tris HCl buffer were combined. The obtained reaction mixture was carefully mixed and then allowed to incubate for 15 min at 37 °C. Subsequently, 100  $\mu$ L of p-Nitrophenyl palmitate solution was

introduced to the reaction mixture, and then the incubation was performed for 35 min at 37 °C. Absorbance measurements were taken using a spectrophotometer at 410 nm. Orlistat served as a standard drug.

#### 2.5.4. Glycation Inhibition

The evaluation of anti-glycation action was performed according to the protocol provided by [40], with minor adjustments. In summary, a mixture was created by combining 25 µL of CL-Eo at various concentrations with 1 mL of hemoglobin solution. Additionally, each tube received 5 µL of gentamicin. Subsequently, 1 mL of a glucose solution at a concentration of 4 mg/mL was introduced to the mixture. The reaction mixture was then incubated in darkness for 72 h. Gallic acid was used as a positive control, and the optical density was read at 443 nm using a spectrophotometer. The calculation of the degree of inhibition of glycation action in the samples was performed using the following formula:

$$\text{Inhibition of glycation (\%)} = [1 - (\text{Abs}_B - ((\text{Abs}_C - \text{Abs}_S) / \text{Abs}_C))] \times 100$$

Abs<sub>B</sub>: Absorbance of hemoglobin in the absence of any sample or glucose.

Abs<sub>C</sub>: Absorbance of hemoglobin combined with glucose.

Abs<sub>S</sub>: Absorbance of a mixture containing hemoglobin, glucose, and the sample (CL-Eo or GA).

### 2.6. Antimicrobial Activity

#### 2.6.1. Microbial Strains

Three bacterial strains, including one Gram-positive bacterium (*Listeria innocua* ATCC 33090) and two Gram-negative bacteria (*Escherichia coli* O157:H7 and *Proteus mirabilis* ATCC 25933), along with two clinical isolates of yeast (*Candida albicans* and *Candida tropicalis*), were evaluated for their susceptibility to CL-Eo. The strains were chosen based on their representation of prevalent pathogenic bacteria linked to human infections and foodborne illnesses. The microbial strains were generously provided by the Laboratory of Microbiology, Rabat. The microorganisms were already identified and categorized at the time of collection in the laboratory. However, in order to maintain the purity and viability of the samples, they were cultivated again on Luria-Bertani (LB) agar for bacteria and yeast extract peptone glucose (YPG) agar for *Candida* species. Subsequently, fresh pure cultures were examined under a microscope using suitable staining methods. Afterward, the cultures were moved to a sterile solution of 0.9% NaCl, and the suspensions were adjusted to a microbial density of 10<sup>6</sup> CFU/mL for bacteria and 10<sup>4</sup> CFU/mL for *Candida* species, using optical density measurements at 625 nm using a UV-visible spectrophotometer. These suspensions were used as working solutions for further microbiological tests.

#### 2.6.2. Disc-Diffusion Test

The antibacterial effectiveness of CL-Eo was estimated using the disc-diffusion technique, following a previously reported methodology with minor modifications [41,42]. The working bacterial and fungal suspensions that were previously prepared and adjusted to 10<sup>6</sup> CFU/mL for bacteria and 10<sup>4</sup> CFU/mL for yeasts, were uniformly spread onto LB agar plates for bacteria and YPG agar plates for *Candida* species using sterile swabs. Sterile filter paper discs with a diameter of 6 mm were saturated with 10 µL of CL-Eo and carefully placed onto the corresponding inoculated plates. Erythromycin 15 µg/disc (for bacteria) and Clotrimazole 20 µg/disc (for yeast) were used as standards. The plates were incubated following adequate conditions for each type of microbial strains, and then, the diameters of the zones of inhibition around each disc were measured in millimeters.

#### 2.6.3. Microdilution Assay for MIC

The minimum inhibitory concentration (MIC) of CL-Eo was measured using a previously published microdilution assay with minor adjustments [42,43]. CL-Eo was diluted in sterile 96-well plates. Each well of a 96-well plate was filled with 95 µL of double-strength

LB broth medium for bacteria or YPG broth for yeast. Serial dilutions of CL-Eo (diluted in 4% DMSO) and the positive control, Erythromycin and were then prepared in separate wells. Subsequently, 10  $\mu$ L of microbial suspensions containing  $10^6$  CFU/mL for bacteria or  $10^4$  CFU/mL were added to the appropriate wells. Then, the microplates were incubated at 35 °C for 18–24 h for bacteria and at 27 °C for 44 h for yeasts. Microbial growth was determined by the addition of 40  $\mu$ L of a 0.2  $\mu$ g/mL solution of TTC to each well and incubated again for 2-h. TTC, which is colorless in its oxidized form, changed to red when reduced by the metabolic activities of the microorganisms. The MIC value is the maximum dilution at which the color change became undetectable.

#### 2.6.4. MBC and MFC Tests

The minimum bactericidal concentration (MBC) and minimum fungicidal concentration (MFC) tests were conducted subsequent to the MIC test, in accordance with a pre-established procedure as indicated by El Hachlafi et al. [32]. During this stage, a pipette was used to transfer 20  $\mu$ L of the solution from each MIC well and evenly distribute it onto Muller–Hinton agar plates. The plates were placed in an incubator following adequate conditions for each type of microbial strain. After the incubation time, the plates were inspected for microbial growth, and a distinct area without any apparent microbial growth indicated the MBC or MFC, which is the lowest concentration of the solution where no microbial growth is seen. The MBC/MIC and MFC/MIC ratios were computed to ascertain the bacteriostatic (fungistatic) or bactericidal (fungicidal) efficacy.

#### 2.7. Antioxidant Activity

The antioxidant potential of CL-Eo was studied through four complementary assays, namely, 2,2'-azino-bis(3-ethylbenzothiazoline-6-sulphonique) (ABTS),  $\beta$ -carotene, 2,2-diphenyl-1-picrylhydrazyl (DPPH) and FRAP tests [41,44]. The results were expressed as  $IC_{50} \pm SD$  of three independent replicates ( $n = 3$ ). BHT and tocopherol were served as standard drugs.

##### 2.7.1. DPPH Assay

The anti-radical activity of CL-Eo was assessed using a modified version of the Villaño et al. method [45] involving the stable radical DPPH. To perform the test, 0.1 mL of CL-Eo, dissolved in ethanol at different concentrations, was mixed with 0.7 mL of a 0.004% DPPH solution. The mixture was then incubated at room temperature in darkness for 25 min. Absorbance was measured at 517 nm. The test was conducted in triplicate, and the  $IC_{50}$  values were derived from the inhibition curves, presented as means  $\pm$  SD.

##### 2.7.2. ABTS Scavenging Assay

The ABTS+ discoloration assay was conducted following established literature methods [46]. In brief, the ABTS+ radical cation was generated by combining equal parts of a 7 mM ABTS solution and a 2.45 mM potassium persulfate solution. This mixture was left in the dark at 25 °C for 14–16 h. The resultant ABTS+ solution was then diluted with methanol to achieve an absorbance of 0.7 ( $\pm 0.03$ ) at 734 nm. Subsequently, 2 mL of the diluted ABTS+ solution was mixed with 200  $\mu$ L of the sample and incubated for 3 min. Absorbance was measured at 734 nm.

##### 2.7.3. FRAP Assay

The reductive potential of CL-Eo was assessed using a slightly modified version of the method described by Benzie and Strain [47]. In short, equal volumes of a 1% potassium ferricyanide  $K_3Fe(CN)_6$  solution and a 0.2 M phosphate buffer solution (pH 6.6) were mixed with CL-Eo at different concentrations. The mixture was then incubated in a water bath at 50 °C for 20 min. To terminate the reaction, 1.25 mL of 10% trichloroacetic acid was added, and the solution was centrifuged at 3500 rpm for 8 min. Subsequently, 1.25 mL of

the supernatant was combined with 1.25 mL of H<sub>2</sub>O<sub>2</sub> and 0.25 mL of 0.1% ferric chloride. Absorbance was measured at 700 nm.

#### 2.7.4. $\beta$ -Carotene Test

The inhibition of lipid peroxidation by CL-Eo was estimated using the  $\beta$ -carotene-linoleic acid test, following the method outlined in [48]. A stock solution of  $\beta$ -carotene/linoleic acid was prepared by dissolving 1 mg of  $\beta$ -carotene in 5 mL of chloroform. To this solution, 10 mg of linoleic acid and 100 mg of Tween-80 were added. The chloroform was then evaporated using a rotary evaporator at 45 °C and 100 rpm. The residue was then dissolved in 50 mL of distilled water. For the assay, 500  $\mu$ L of the  $\beta$ -carotene solution was mixed with 50  $\mu$ L of CL-Eo at various concentrations. The mixtures were incubated in boiling water at 50 °C for 100 min. The change in  $\beta$ -carotene absorbance was measured at 470 nm against a blank.

#### 2.8. Statistical Analysis

All tests were conducted in three independent replicates, and the resulting data are presented as mean  $\pm$  SD. Statistical analysis was performed using GraphPad 9, and mean comparisons were executed through one-way analysis of variance (ANOVA) followed by the Tukey test.

### 3. Results and Discussion

#### 3.1. GC-Characterization of CL-Eo

The yield of CL-Eo obtained by MHD of aerial parts is  $4.15 \pm 0.03$  (% *v/w*), which is higher than those of *C. ladanifer* oil extracted by traditional hydrodistillation (ranging from 0.3 to 0.4% (mL per 100 g of plant)) [49].

The results of the GC-MS characterization of CL-Eo allowed the identification of twenty-four components, representing 99.37% of total Eo (Figure 1). Table 1 presents all identified components and their quantification using the percentage of relative area. It is observed that oxygenated monoterpenes (55.29%) and monoterpene hydrocarbons (36.3%) were the principal phytochemical groups in the analyzed Eo. In fact, the main constituents were linderol (17.76%), gamma-terpinene (17.55%), borneol (13.78%), carvacrol (7.93%), caryophyllene (7.01%), and camphene (6.52%) (Figure 2).

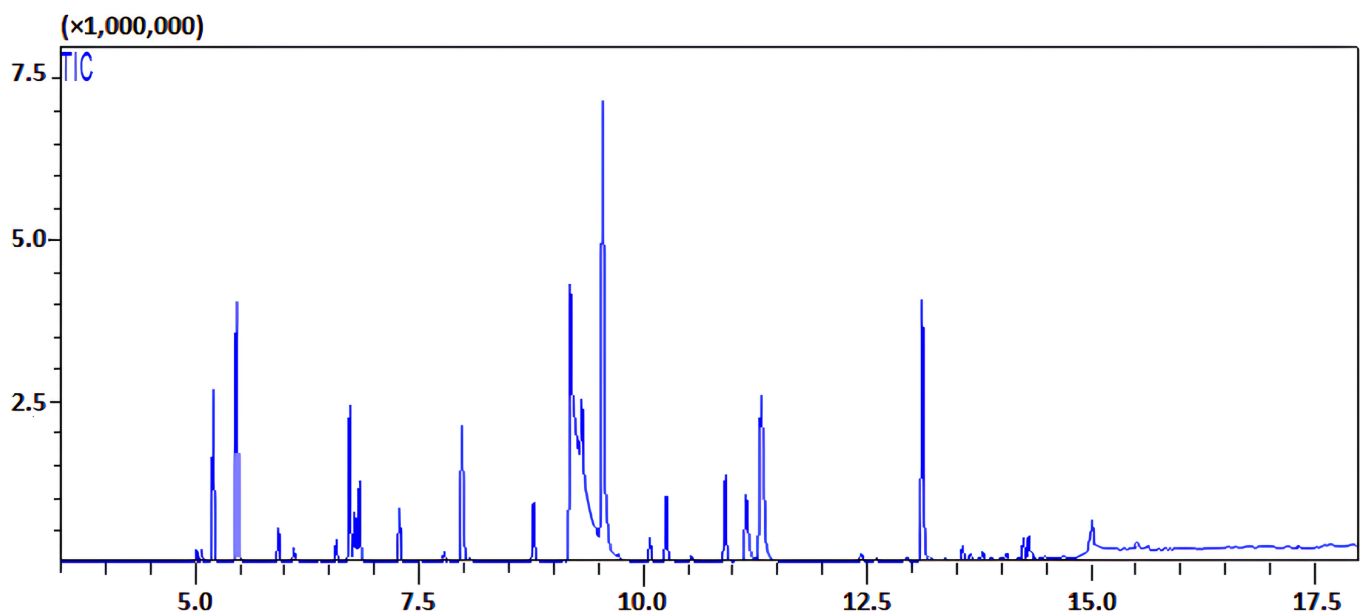
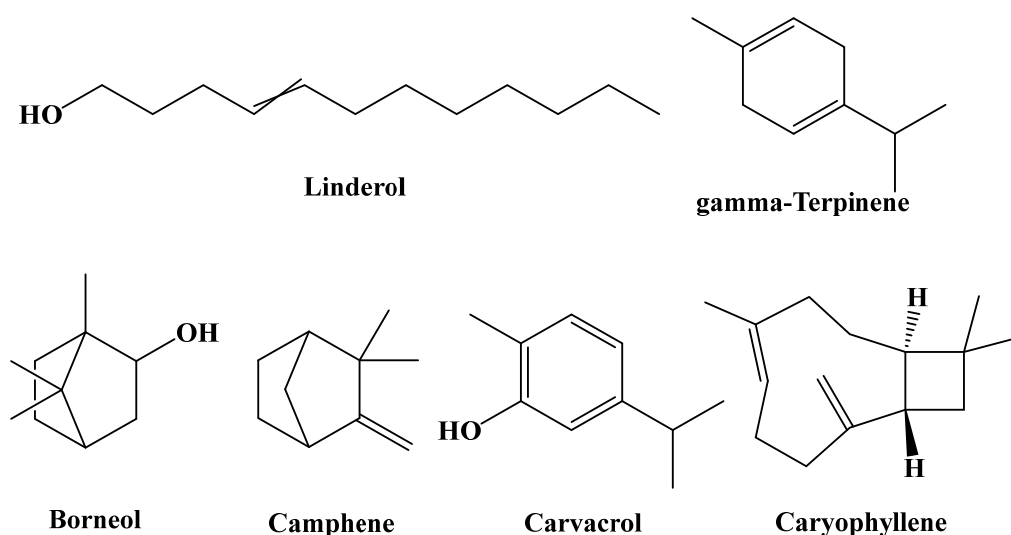


Figure 1. Chromatogram of gas chromatography (GC) analysis of CL-Eo.

**Table 1.** Volatile constituents identified in CL-Eo.

N.pic	Compounds	Formula	MW (g/mol)	T (min)	% Area
1	Tricyclene	C <sub>10</sub> H <sub>16</sub>	136.23	5.015	0.30
2	alpha-Thujene	C <sub>10</sub> H <sub>16</sub>	136.23	5.072	0.26
3	alpha-Pinene	C <sub>10</sub> H <sub>16</sub>	136.23	5.201	3.76
4	Camphene	C <sub>10</sub> H <sub>16</sub>	136.23	5.463	6.52
5	Sabinene	C <sub>10</sub> H <sub>16</sub>	136.23	5.928	0.86
6	beta-pinene	C <sub>10</sub> H <sub>16</sub>	136.23	6.101	0.34
7	(+)-4-Carene	C <sub>10</sub> H <sub>16</sub>	136.23	6.575	0.52
8	beta-Cymene	C <sub>10</sub> H <sub>14</sub>	134.22	6.724	4.62
9	D-Limonene	C <sub>10</sub> H <sub>16</sub>	136.23	6.783	1.30
10	Eucalyptol	C <sub>10</sub> H <sub>18</sub> O	154.25	6.832	2.02
11	2-Carene	C <sub>10</sub> H <sub>16</sub>	136.23	7.777	0.27
12	beta.-Linalool	C <sub>10</sub> H <sub>18</sub> O	154.25	7.977	3.96
13	Camphor	C <sub>10</sub> H <sub>16</sub> O	152.23	8.777	1.73
14	Linderol	C <sub>10</sub> H <sub>18</sub> O	154.25	9.187	17.76
15	Borneol	C <sub>10</sub> H <sub>18</sub> O	154.25	9.315	13.78
16	gamma-Terpinen	C <sub>10</sub> H <sub>16</sub>	136.23	9.550	17.55
17	alpha.-Citral	C <sub>10</sub> H <sub>16</sub> O	152.23	10.076	0.63
18	Thymol methyl ether	C <sub>10</sub> H <sub>16</sub> O	164.24	10.259	1.84
19	p-Cumic aldehyde	C <sub>10</sub> H <sub>12</sub> O	148.2	10.543	0.21
20	Isoborneol, acetate	C <sub>12</sub> H <sub>20</sub> O <sub>2</sub>	196.29	10.916	2.30
21	Thymol	C <sub>10</sub> H <sub>14</sub> O	150.22	11.150	3.11
22	Carvacrol	C <sub>10</sub> H <sub>14</sub> O	150.22	11.318	7.93
23	Caryophyllene	C <sub>15</sub> H <sub>24</sub>	204.35	13.118	7.06
24	Cedr-8-ene	C <sub>15</sub> H <sub>24</sub>	204.35	14.306	0.74
Yield (% , <i>v/w</i> )				4.15 ± 0.03	
<b>Total identified (%)</b>					99.37
Monoterpene hydrocarbons					36.3
Oxygenated monoterpenes					55.29
Sesquiterpene hydrocarbons					7.80
Oxygenated sesquiterpenes					-
Other					-



**Figure 2.** Most abundant volatile compounds in CL-Eo.

In fact, the biological properties of CL-Eo are probably attributed to its main component, such as gamma-terpinene, borneol, carvacrol and camphene, which exhibit a variety of pharmacological activities. Borneol and carvacrol have neutralized the reactive oxygen species (ROS) and reduced oxidative stress [50]. Moreover, they also showed antimicrobial



activity against various pathogens, including bacteria and fungi [51]. This suggests their potential application in treating infections and as a natural preservative in food and cosmetic industries. Gamma-terpinene has shown to inhibit inflammatory pathways by inhibiting key enzymes and cytokines involved in inflammation [52]. Camphene modulated the activity of enzymes related to liver function and cardiovascular health and can trigger cell death in cancer cells via apoptosis, making it a potential candidate for cancer therapy [53]. It has been reported to possess anti-inflammatory properties, reducing the production of pro-inflammatory cytokines and mediators [53].

However, previous studies on CL-Eo have revealed significant variation in their chemical composition. For instance, a study conducted in the province of Taza (Morocco) identified viridiflorol (28.82%),  $\gamma$ -gurjunene (14.61%), and cadina-1,4-diene (5.87%) as the main compounds of CL-Eo [22]. Similarly, research in the province of Khemissetla (Morocco) highlighted the presence of viridiflorol (17.74%), trans-pinocarveol (11.02%), and ledol (8.85%) as the main compounds of CL-Eo [54]. In a study conducted in Spain, Pérez et al. [55] identified four major compounds in CL-Eo, namely  $\alpha$ -pinene, (E)-pinocarveol, viridiflorol, and ledol. Similarly, a study by Verdeguer et al. (2012) on *C. ladaniferus* in San Lorenzo del Escorial, Spain, identified trans-pinocarveol (20.00%), viridiflorol (13.59%), bornyl acetate (7.03%), and  $\alpha$ -pinene (4.70%) as the main volatile compounds [56]. Differences in the oil compositions found in this study compared to those reported in other research can be attributed to a variety of factors, including ecological conditions, genetic variations, environmental influences, geographical origins, and the season in which the plant was harvested [57]. Indeed, the location's latitude and altitude can influence temperature, sunlight, and growing season, all affecting oil composition. Moreover, the surrounding plant biodiversity can affect oil composition through interactions with local ecosystems [17]. Traditional agricultural practices in different regions can influence how plants are grown, harvested, and processed, impacting oil quality [21]. For instance, the chemical constituents of CL-Eo from Portugal indicated the dominance of other compounds, such as sesquiterpenes alcohols, viridiflorol (13.6–17.4%), globulol (3.1–5.0%) [58]. In addition, the composition of CL-Eo cultivated in central Spain, reported its richness in monoterpenes, with trans-pinocarveol (20.01%), bornyl acetate (7.0%), and 4-Terpineol (6.30%) as major compounds [54]. On the other hand, the season of harvest of the plant may significantly impact its oil composition. In fact, the maturity of the plant at harvest can greatly influence oil content and composition [21]. Younger plants might have different oil profiles compared to mature plants. Moreover, seasonal changes in temperature and daylight can affect oil synthesis, leading to variations in composition depending on the harvest time. Additionally, different seasons can induce changes in plant physiology and metabolism, affecting oil characteristics.

### 3.2. Molecular Docking Analysis

Molecular docking, a highly efficient computational methodology, is commonly utilized to obtain significant insights into the molecular mechanisms of pharmacologically active medications [59,60]. In this study, molecular docking has been employed to examine the probable mechanism behind the anti-inflammatory activities exhibited by the components of CL-Eo. The study attempted to ascertain if the studied compounds displayed a greater or lesser affinity towards a certain target protein in contrast to a known inhibitor (native ligand) by analyzing binding affinity values. Generally, a reduction in binding energy indicates a rise in compound affinity. In order to effectively display the docking scores, a table with a heat-map format has been utilized, employing a three-color scheme consisting of red, yellow, and green. The color spectrum ranged from the lowest energy values, depicted in red (often related to the docking score of the native ligand), to the greatest energy values, depicted in green. This method enabled the discovery of chemical compounds that could potentially act as inhibitors by comparing their lowest values to those of the native ligand for a given protein.

The main objective of this approach was to assess the binding of 14 key constituents of Eo (which make up over 90% of the total composition) to specific target proteins involved in tyrosinase inhibition, diabetes, and inflammation. The target proteins in question are tyrosinase [31],  $\alpha$ -amylase [33],  $\alpha$ -Glucosidase [34], pancreatic lipase [35], lipoxygenase (LOX) [29]. These proteins have been identified by their respective PDB IDs: 5I3B, 1SMD, 5NN5, 1LPB, and 1N8Q.

### 3.2.1. Prediction of the Dermatoprotective Activity of the Major Compounds in CL-Eo

Tyrosinase serves as the principal regulatory enzyme within the melanin biosynthesis pathway, playing a central role, particularly in the initial stages of the process. This enzymatic catalyst holds a pivotal position in overseeing the crucial steps involving the conversion of tyrosine into 3,4-dihydroxyphenylalanine (DOPA) and the subsequent oxidation of DOPA to dopaquinone [61]. Throughout the intricate cascade of melanin production, tyrosinase’s influence is notably pronounced during these fundamental stages, underscoring its significant contribution to the synthesis of melanin—the pigment responsible for determining skin, hair, and eye coloration. The enzymatic activities related to converting tyrosine to DOPA and the subsequent oxidation of DOPA to dopaquinone emerge as integral components of this finely regulated biological pathway, emphasizing the indispensable role played by tyrosinase in the intricate process of melanin biosynthesis.

In the course of investigating docking interactions and conducting calculations for binding free energy,  $\beta$ -cymene exhibited the most significant interaction energy with tyrosinase (PDB ID: 5I3B), registering at  $-5.8$  kcal/mol. Notably, this outcome was observed among the 14 ligands evaluated, in contrast to the native tyrosinase inhibitor, hydroquinone, which displayed a binding free energy of  $-5.5$  kcal/mol. Illustrated in Figure 3A,  $\beta$ -cymene demonstrated several interactions within the active site of tyrosinase, primarily with crucial amino acid residues forming the binding pocket, including Gly143, Ile139, Ala44, Tyr267, and Lys47, among others—a pattern consistent with the interactions observed for the native ligand hydroquinone (Figure 3B).

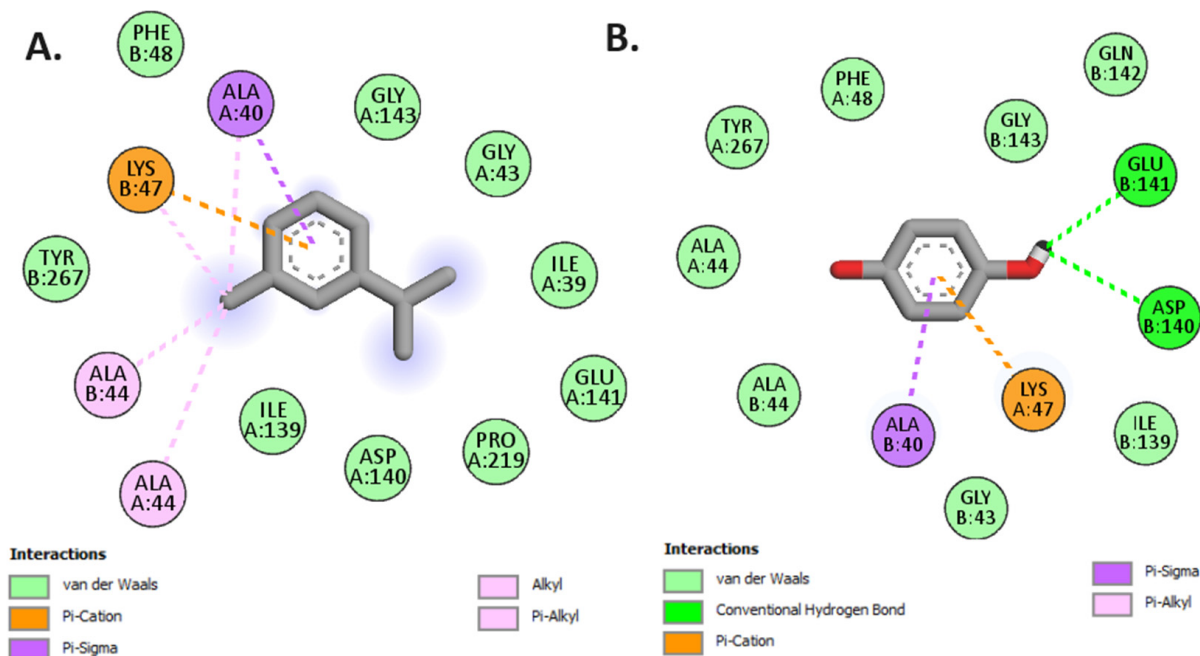


**Figure 3.** The 2D molecular docking interactions of  $\beta$ -cymene (A), and hydroquinone (B) (native ligand of Tyr), with tyrosinase (PDB: 5I3B).

### 3.2.2. Prediction of the Anti-Inflammatory Activity of the Major Compounds in CL-Eo

Lipoxygenases (LOXs) have a broad distribution in nature and are plentiful in both plants and mammals [62]. The main function of these enzymes is to target polyunsaturated fatty acids (PUFA) that have cis double bonds. Arachidonic acid (AA), a 20-carbon compound, is commonly found as a substrate in mammals [62]. LOX enzymes are designated according to the specific carbon they oxygenate. Instances of lipoxygenase enzymes found in plants include 9-LOX and 13-LOX, while animals possess 5-LOX, 12-LOX, and 15-LOX [63]. Lipoxygenases (LOXs) are essential enzymes that contribute significantly to several biological processes through the generation of hydroperoxides. These hydroperoxides serve as precursors for crucial signaling molecules and biological mediators [64]. Nevertheless, LOX-catalyzed processes might potentially result in unfavorable consequences.

In the course of the present investigation, the authors have conducted assessments of the binding affinities and interactions between the selected ligands and the target protein to delineate their inhibitory potential. Among the 14 compounds examined, five exhibited lower docking score values, varying between  $-6$  and  $-6.5$  kcal/mol, indicating a heightened inhibitory potential in comparison to the native ligand protocatechuic acid, which registered a score of  $-5.9$  kcal/mol. Particularly noteworthy was the substantial binding affinity of caryophyllene, attaining a score of  $-6.5$  kcal/mol (refer to Table 2). To contextualize these outcomes, the authors have juxtaposed them with the binding affinity of the native ligand, protocatechuic acid. Caryophyllene's interaction with the protein implicated an alkyl interaction with a precise amino acid residue, Ala263. Importantly, when contrasting these results with those of the native ligand, it was noticed that the native ligand formed seven hydrogen bonds, as depicted in Figure 4. These outcomes underscore the capacity of caryophyllene as an inhibitor of the target protein, and the diverse nature of its binding interactions highlights their promise for its use in drug discovery.

**Table 2.** Heat map of the docking scores (binding free energy values are expressed in kcal/mol) of *C. ladanifer* essential oils components: 1N8Q: lipoxygenase (LOX); 5I3B: tyrosinase; 5NN5:  $\alpha$ -glucosidase; 1SMD:  $\alpha$ -amylase, 1LPB: pancreatic lipase.

N°	Compounds	5I3B	1N8Q	5NN5	1SMD	1LPB
		(Dermatoprotecti)	(Anti-Inflammatory)		(Anti-Diabetic)	
Free Binding Energy (Kcal/mol) *						
-	Native Ligand	-5.5	-5.9	-7.4	-7.8	-7.8
1	Linderol	-4.6	-6.2	-5.3	-5.5	-5
2	$\gamma$ -Terpinene	-4.6	-6.4	-7	-5.3	-5.1
3	Borneol	-5	-5.7	-5.2	-5.5	-5.1
4	Carvacrol	-5.1	-6	-5.8	-6.4	-5.6
5	Caryophyllene	-5.3	-6.5	-5.7	-7.8	-7.9
6	Camphene	-4.6	-6.1	-5.3	-5.5	-5
7	$\beta$ -Linalool	-4.4	-4.7	-5.1	-5	-5
8	$\alpha$ -Pinene	-4.8	-5.6	-5.2	-5.4	-5.1
9	$\beta$ -Cymene	-5.8	-5.4	-6.2	-5.7	-5.6
10	Thymol	-5	-5.6	-5.7	-5.9	-5.8
11	Isoborneol, acetate	-5.3	-5.8	-5.4	-6	-5.4
12	Eucalyptol	-4.8	-5.1	-5.4	-5.4	-5.1
13	Thymol methyl ether	-5.1	-5.2	-5.4	-5.4	-5.4
14	Camphor	-5	-5.3	-5.6	-5.4	-5.1

\* For each column, the color scale ranges from red (referring to the native ligand  $\Delta G$ ), through yellow (mid-point at 50% centile), to green (native ligand  $\Delta G + 4$  kcal/mol).

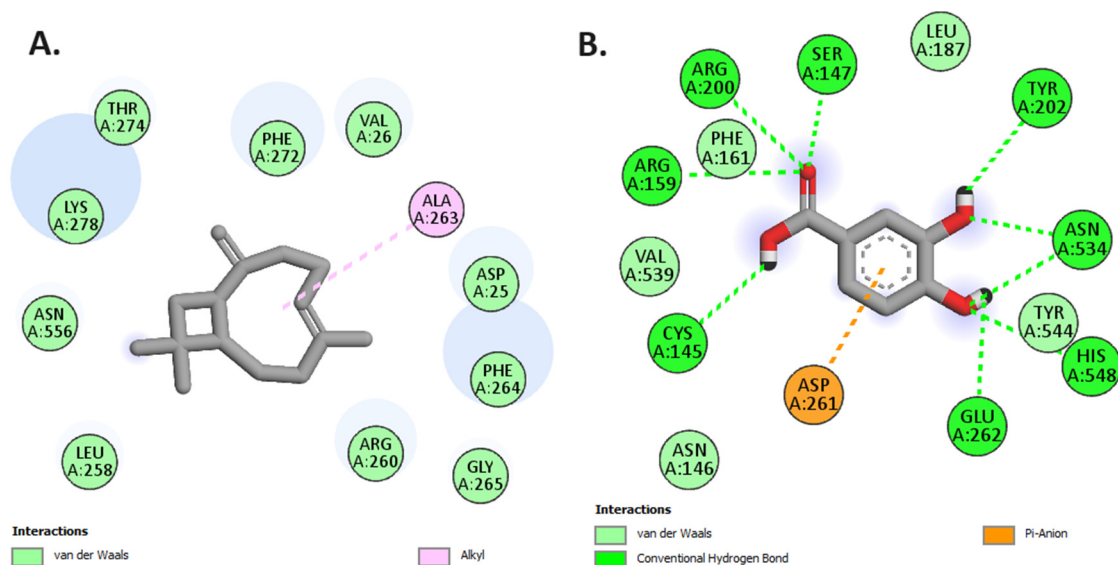


**Figure 4.** The 2D molecular docking interactions of Caryophyllene (A), and protocatechuic acid (native ligand of lipoxigenase) (B), with lipoxigenase (PDB: 1N8Q).

### 3.2.3. Prediction of the Antidiabetic Activity of the Major Compounds in CL-Eo

#### - $\alpha$ -glucosidase inhibitory activity

$\alpha$ -glucosidase is an essential digestive enzyme that plays a key role in accelerating the digestion of polysaccharides, specifically starch, into glucose by breaking (14) bonds. This mechanism enhances the uptake of glucose, ultimately resulting in elevated levels of glucose in the bloodstream [65,66]. This enzyme regulates the breakdown of starch and other carbs in the diet, which helps avoid high blood sugar levels and maintain appropriate blood sugar levels [65,66].  $\alpha$ -glucosidase greatly increases the uptake of simple sugars, such as glucose, obtained from starch and dietary carbohydrates in the intestines, leading to higher amounts of glucose in the bloodstream [67].

Among all the evaluated ligands, none displayed a significant affinity for the enzyme's active site (PDB ID: 5NN5), exhibiting lower binding energies with docking scores ranging from  $-5.1$  to  $-6.2$  kcal/mol when compared to that of the native ligand (acarbose;  $-7.4$  kcal/mol). Notably,  $\gamma$ -terpinene exhibited a docking score close to that of the native ligand, suggesting a potential worth exploring, even though it did not display notable interactions with the binding site (see Figure 5). However, it is plausible that the inhibitory potential of CL-Eo compounds may stem from a synergistic activity among the compounds in inhibiting the enzyme's activity.

#### - $\alpha$ -amylase inhibitory activity

$\alpha$ -amylase acts as a catalyst by breaking down  $\alpha$ -linked polysaccharides into  $\alpha$ -anomeric products through hydrolysis [68]. This enzyme is essential for the process of breaking down carbohydrates. It is found and functions in both pancreatic juice and saliva [69]. The  $\alpha$ -amylase's active site, identified by PDB ID: 1SMD, consists of three catalytic residues: Asp197, Glu233, and Asp300. In addition, the enzyme's activity is considerably influenced by numerous additional residues, namely Arg337, Arg195, Asn298, Phe265, Phe295, His201, Ala307, Gly306, Trp203, Trp284, Trp59, Tyr62, Trp58, His299, and His101 [69–71].

Among the various tested ligands, only one, namely caryophyllene, demonstrated an affinity equivalent to that of the native ligand (acarbose;  $-7.8$  kcal/mol) for the active site. Caryophyllene was observed to engage in van der Waals interactions with amino acid residues, namely Trp59, Trp58, Tyr62, and Gly306, which could potentially impact the enzyme's activity (refer to Figure 6A). A similar pattern was observed with the potent inhibitor, acarbose, which exhibited a notable number of interactions within the binding

pocket of the enzyme (Figure 6B). These findings underscore the potential of caryophyllene in inhibiting  $\alpha$ -amylase activity.

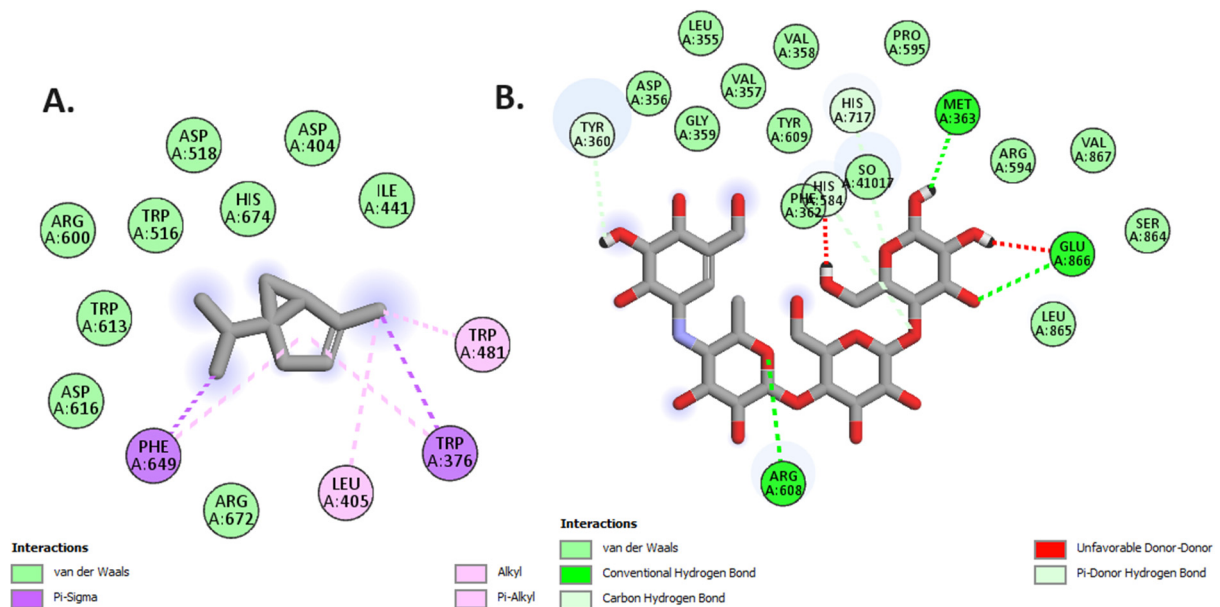


**Figure 5.** The 2D molecular docking interactions of  $\gamma$ -terpinene (A), and acarbose (B) (potent inhibitor of  $\alpha$ -glucosidase), with  $\alpha$ -glucosidase enzyme (PDB: 5NN5).

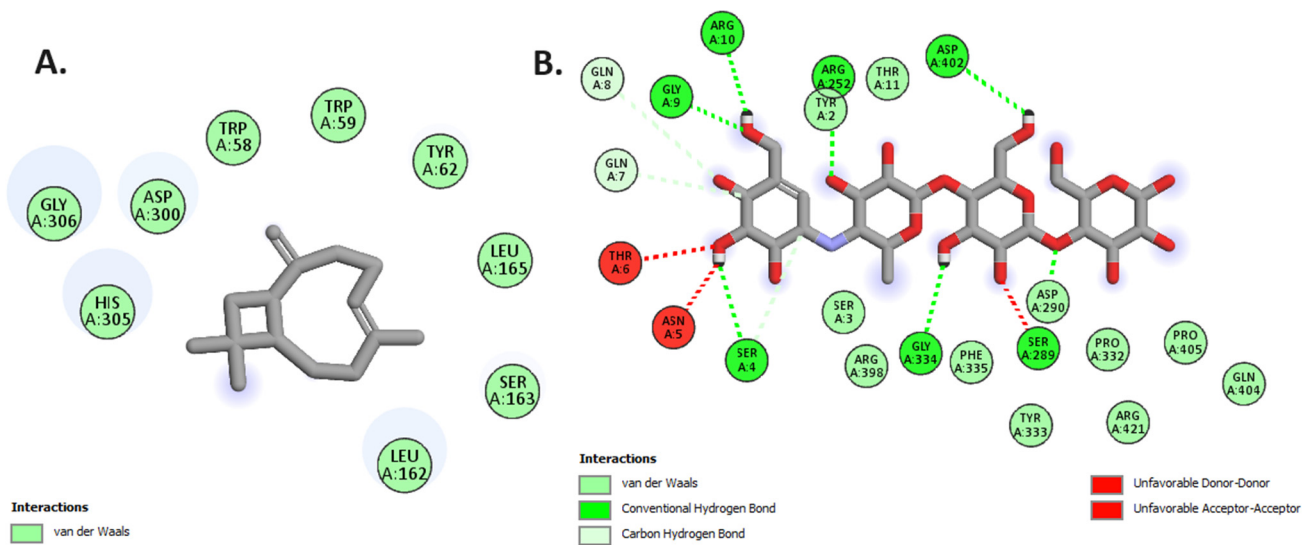


**Figure 6.** The 2D molecular docking interactions of caryophyllene (A), and acarbose (B) (potent inhibitor of  $\alpha$ -amylase), with  $\alpha$ -amylase enzyme (PDB: 1SMD).

- Lipase pancreatic

Inhibition of human pancreatic lipase, a pivotal enzyme essential for the digestion and absorption of dietary fats, represents a potent therapeutic strategy in the treatment of obesity [72]. The modulation of pancreatic lipase activity is instrumental in controlling the breakdown of triglycerides into free fatty acids and glycerol, thereby influencing the overall absorption of fats in the digestive system [72]. This targeted intervention not only holds promise for combating obesity by reducing the absorption of dietary fats but also has potential implications in the context of diabetes [72]. Obesity is intricately linked to the development of type 2 diabetes, as excess body fat contributes to insulin resistance and impaired glucose metabolism.

Of the numerous ligands subjected to testing, only one displayed an affinity comparable to that of the potent lipase inhibitor, orlistat (with a binding free energy of  $-7.8$  kcal/mol), for the active site. Caryophyllene manifested the highest affinity among these ligands, recording a value of  $-7.9$  kcal/mol. This interaction involved one alkyl interaction with the amino acid residue Lys42, along with seven van der Waals interactions with amino acid residues within the binding pocket (Figure 7). These findings suggest caryophyllene as a prospective pancreatic lipase inhibitor, warranting an in-depth investigation.

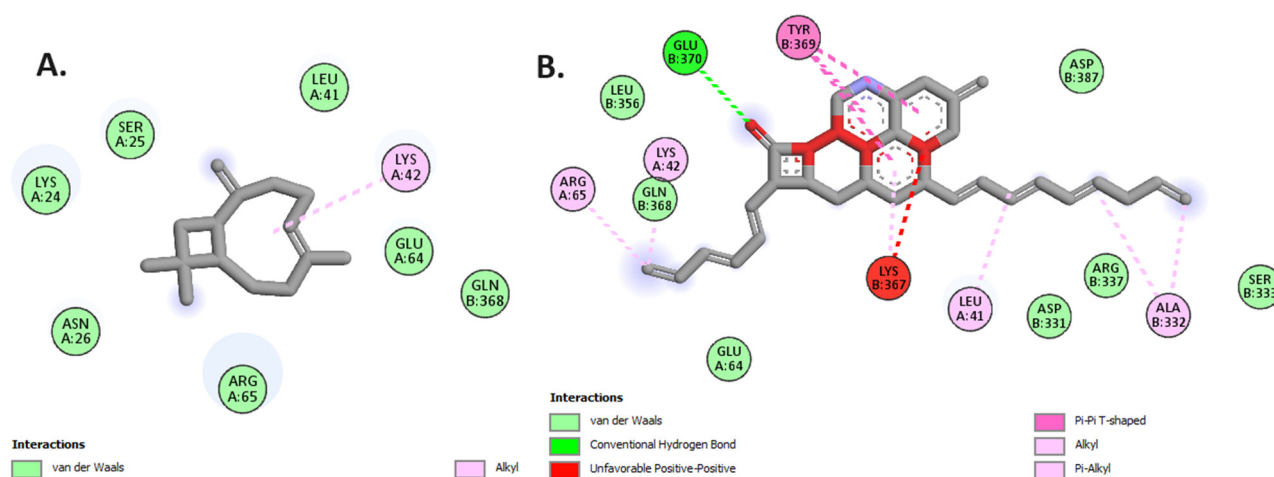


**Figure 7.** The 2D molecular docking interactions of caryophyllene (A), and orlistat (B) (potent inhibitor of lipase), with pancreatic lipase (PDB: 1LPB).

In summary, the compounds derived from CL-Eo have demonstrated noteworthy efficacy in targeting prominent enzymes such as tyrosinase, lipoxygenase,  $\alpha$ -amylase, and pancreatic lipase, with  $\beta$ -cymene and caryophyllene emerging as significant ligands. These observations present promising opportunities for continued research and the development of therapeutic agents designed to address diabetes and inflammation-related disorders. The intricate interactions between Eo compounds and these protein targets offer valuable insights for future investigations, potentially paving the way for innovative treatments.

### 3.3. In Vitro Biological Investigations

#### 3.3.1. In Vitro Inhibition of $\alpha$ -Amylase and $\alpha$ -Glucosidase Enzymes

The current assessment of antidiabetic activity involves measuring the inhibition of  $\alpha$ -amylase and  $\alpha$ -Glucosidase. The results of the inhibitory effects of CL-Eo and acarbose on this enzyme  $\alpha$ -amylase in vitro are depicted in Figure 8a. In accordance with Figure 8a, CL-Eo significantly influenced the effect of pancreatic  $\alpha$ -amylase in a dose-dependent manner ( $p < 0.001$ ). At a higher concentration of 1 mg/mL, CL-Eo demonstrated an inhibition percentage of 86.17%, with an  $IC_{50}$  value of approximately  $0.41 \pm 0.009$  mg/mL (Figure 8b). Furthermore, CL-Eo exhibited a similar effect on pancreatic  $\alpha$ -amylase enzyme compared to the reference molecule acarbose, with an  $IC_{50}$  value of  $0.42 \pm 0.007$  mg/mL.

On the other hand, the CL-Eo exhibits a highly significant inhibitory activity against intestinal  $\alpha$ -glucosidase enzyme ( $p < 0.001$ ), with an inhibition percentage of 84.66% (Figure 9a). These outcomes were confirmed by the recorded  $IC_{50}$  values for CL-Eo and acarbose, which were  $0.49 \pm 0.002$  mg/mL and  $0.38 \pm 0.003$  mg/mL, respectively (Figure 9b). Consistent with these findings, the use of this oil prevents the formation of monosaccharides, thereby avoiding an increase in blood glucose levels.

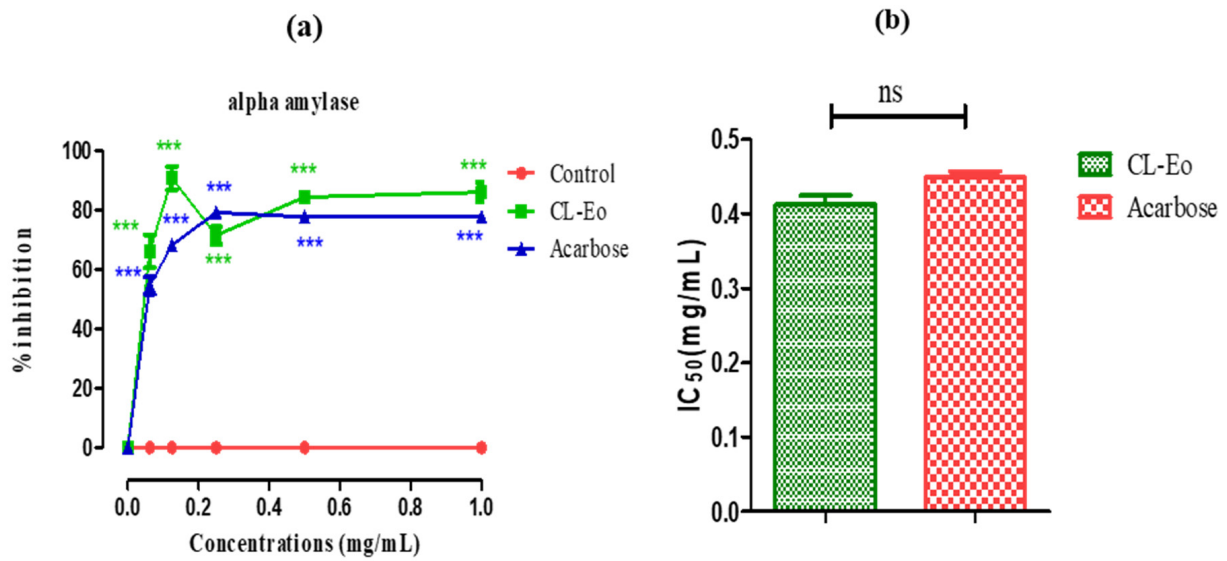


**Figure 8.** Inhibitory effect (a) and IC<sub>50</sub> values (mg/mL) (b) on pancreatic  $\alpha$ -amylase enzymes through CL-Eo and acarbose in vitro. The values are the means  $\pm$  SEM ( $n = 3$ ). \*\*\*  $p < 0.001$  as a function of the control group, ns: no significant.

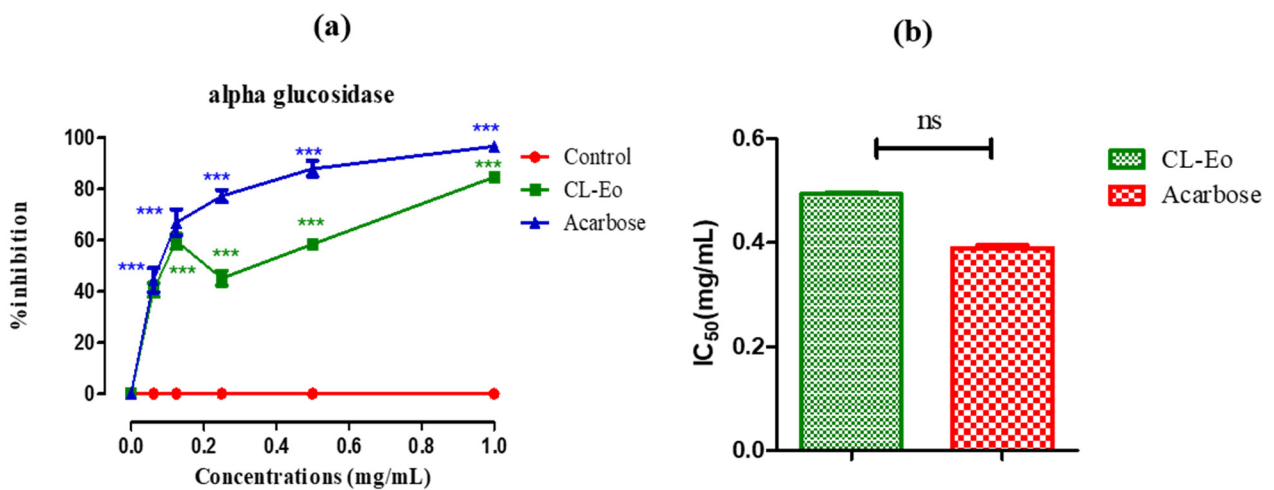


**Figure 9.** Inhibitory effect (a) on intestinal  $\alpha$ -glucosidase enzyme through CL-Eo and acarbose in vitro (b) and IC<sub>50</sub> values (mg/mL). The values are the means  $\pm$  SEM ( $n = 3$ ). \*\*\*  $p < 0.001$  as a function of the control group, ns: not significant.

Several species of *Cistus* have been assessed for their inhibitory effects on the activities of  $\alpha$ -amylase and  $\alpha$ -glucosidase [73–75]. However, research conducted by Sayah et al. [74] on extracts of *C. salviifolius* and *C. monspeliensis* demonstrated that these plants exhibited inhibition of  $\alpha$ -amylase (IC<sub>50</sub> = 217.10 and 886.10  $\mu$ g/mL, respectively) and  $\alpha$ -glucosidase (IC<sub>50</sub> = 0.95 and 14.58  $\mu$ g/mL, respectively) [74]. Another study on aqueous and ethanolic extracts of *C. salviifolius* showed that these extracts inhibited  $\alpha$ -amylase with IC<sub>50</sub> values of 17.59 and 3.46  $\mu$ g/mL, respectively, as well as  $\alpha$ -glucosidase (IC<sub>50</sub> = 0.33 and 0.098  $\mu$ g/mL, respectively) [75].

Regarding the compounds identified by GC-MS in CL-Eo, previous studies have demonstrated the role of monoterpenes as key inhibitors of  $\alpha$ -amylase and  $\alpha$ -glucosidase [76,77]. In Tan et al.'s work [76], the inhibition of  $\alpha$ -amylase and  $\alpha$ -glucosidase activities was evaluated for several classes of monoterpenes. Among those identified in *C. ladaniiferus*, citral showed an inhibitory potential on  $\alpha$ -amylase of 45.7%, at a concentration of 10 mM, while limonene exhibited the strongest inhibitory effect on  $\alpha$ -glucosidase activity, with a percentage of 21.3%.

Other research conducted by Kaur et al. [78] demonstrated that caryophyllene inhibited  $\alpha$ -glucosidase by 50% at a concentration of 80  $\mu\text{g}/\text{mL}$  [78]. Aazza et al. [79] indicated that carvacrol displays a key role in the inhibition of  $\alpha$ -amylase [79]. In fact, it has also been noted that carvacrol significantly attenuates the enzymatic activity of  $\alpha$ -amylase [80].

### 3.3.2. In Vitro Inhibition of Pancreatic Lipase Enzyme

Obesity refers to a condition where the body accumulates an excess of fat, thereby increasing the risk of various diseases, including diabetes [81]. It is characterized by the excessive storage of fat in the body. Weight loss can be achieved by inhibiting fat absorption, which involves regulating the activity of pancreatic lipase, a crucial enzymatic element in the metabolic process of fats [82]. Orlistat is one of the most commonly used medications to inhibit lipase, blocking approximately 30% of the absorption of exogenous fat. However, it comes with undesirable side effects such as diarrhea and abdominal cramps [83]. Since ancient times, natural resources have played a significant role, and currently, scientific research is focused on validating and improving these therapeutic effects. In the context of this study, the effect of CL-Eo on the inhibition of pancreatic lipase enzymes is also significant ( $p < 0.001$ ), with an inhibition percentage of 89.91% (Figure 10a). These results were supported by the  $\text{IC}_{50}$  values recorded for CL-Eo and orlistat, which were, respectively,  $0.45 \pm 0.004 \text{ mg}/\text{mL}$  and  $0.49 \pm 0.0007 \text{ mg}/\text{mL}$  (Figure 10b).

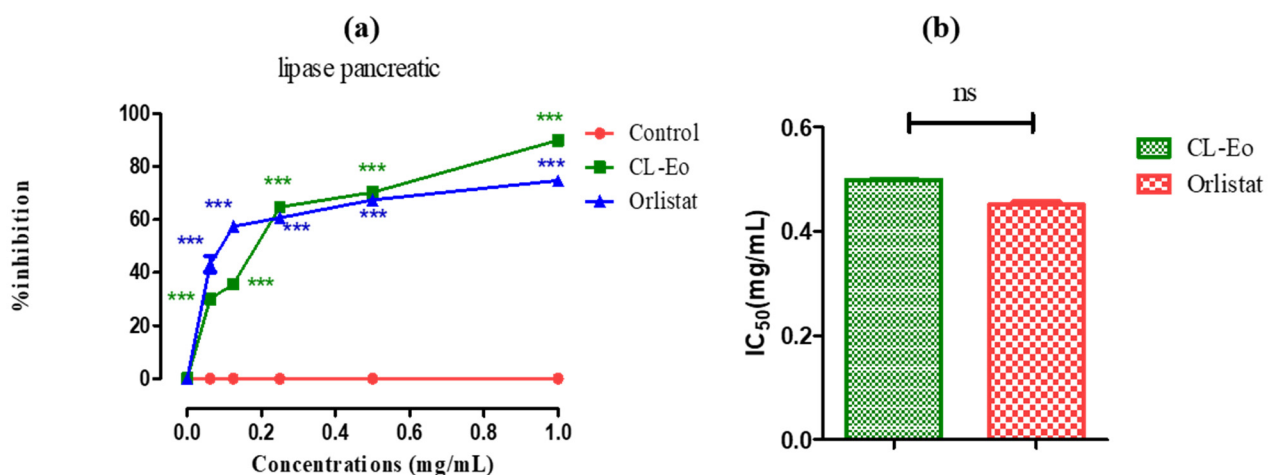


**Figure 10.** Porcine pancreatic lipase inhibitory activity (a) and  $\text{IC}_{50}$  values (mg/mL) (b) of CL-Eo and Orlistat. Data were presented as mean  $\pm$  SEM ( $n = 3$ ). \*\*\*  $p < 0.001$  as a function of the control group, ns: not significant.

The results of inhibition of pancreatic lipase by *C. ladaniferus* are not available in the literature. Therefore, this investigation reports for the first time the inhibitory activity of this plant species on pancreatic lipase enzymes.

### 3.3.3. Glycation Inhibition

Glycation is a process where reducing sugars react with the amino groups in proteins. This reaction first creates a reversible Schiff base, which can then change into an Amadori product [84]. The latter undergoes further structural modifications and may eventually result in the establishment of advanced glycation end products, playing a significant role in diabetes-related complications [85]. The inhibitory capacity of glycation by CL-Eo was evaluated in the context of BSA glycation. The discovery of new glycation inhibitors, aimed at preventing the formation of advanced glycation end products (AGEs), is particularly important due to their association with diabetes complications. The results highlighted a significant inhibition of hemoglobin glycation activity by CL-Eo compared to the control group ( $p < 0.001$ ). Specifically, CL-Eo exhibited its maximum activity at a concentration of 0.5 mg/mL, reaching 84.86% (Figure 11a). The  $\text{IC}_{50}$  value of CL-Eo attests to its remarkable



antiglycation activity, standing at  $0.32 \pm 0.006$  mg/mL. Additionally, gallic acid (GA) revealed the highest antiglycation action, reaching 87.35% at a concentration of 0.25 mg/mL ( $p < 0.001$ ), with an  $IC_{50}$  value measured at  $0.41 \pm 0.003$  mg/mL (Figure 11b). These results underscore the antiglycation potential of CL-Eo, positioning GA as a standard.

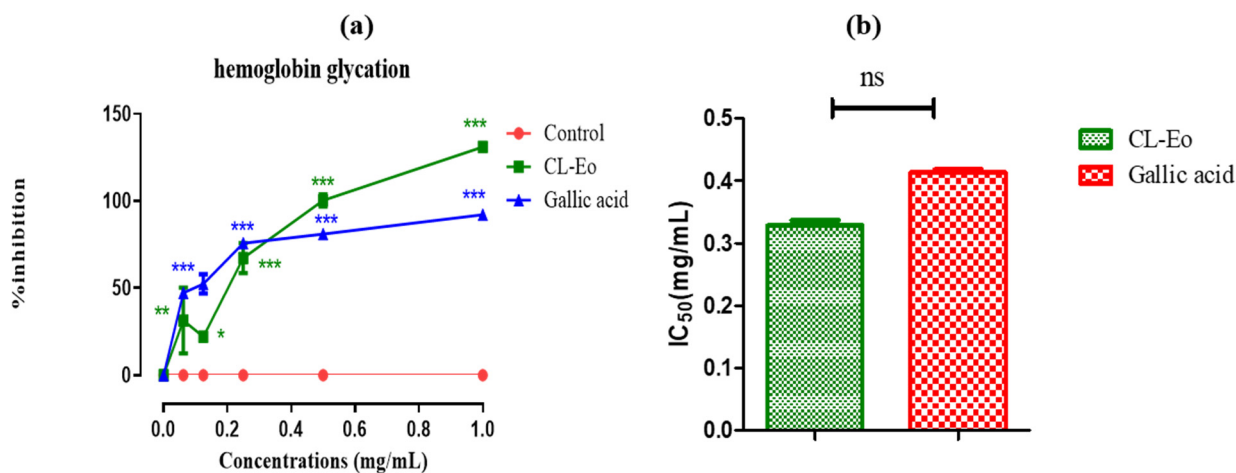


**Figure 11.** Inhibitory effect on glycation activity of hemoglobin (a) and  $IC_{50}$  values (mg/mL) (b) of CL-Eo and gallic acid. Results are shown as mean  $\pm$  SM ( $n = 3$ ). \*  $p < 0.05$ , \*\*  $p < 0.01$ , \*\*\*  $p < 0.001$  as a function of the control group, ns: not significant.

The results of glycation inhibition by *C. ladaniferus* are not available in the literature. Therefore, the authors have compared them to those of other *Cistus* species. A comparative study conducted by İnan et al. [86] on the aqueous extract of different *Cistus* species, namely *C. creticus*, *C. laurifolius*, *C. monspeliensis*, *C. parviflorus*, and *C. salvifolius*, showed glycation inhibition ranging from 69.60% to 84.26% [73]. Another study focusing on five flavonoid compounds from *C. incanus* demonstrated anti-glycation potential, particularly for hyperoside ( $78 \pm 0.8\%$ ), quercetin ( $76.8 \pm 10.8\%$ ), kaempferol ( $56.3 \pm 3.6\%$ ), myricitrine ( $51.3 \pm 3.5\%$ ), and myricetin ( $23 \pm 5.6\%$ ) [86].

### 3.3.4. Antimicrobial Activity

The antibacterial activity of CL-Eo showed significant variation among the bacterial strains, as shown in Table 3. *P. mirabilis* exhibited the greatest susceptibility, with an inhibition zone of  $17.16 \pm 1.04$  mm. Following that, *L. innocua* displayed an inhibition zone of  $13.48 \pm 1.65$  mm, whereas *E. coli* had an inhibition zone measuring  $12.47 \pm 0.61$  mm. Significant differences in the inhibitory zones of all studied bacteria, except for *L. innocua*, were observed when compared to the control antibiotic, Erythromycin.

**Table 3.** Evaluation of CL-Eo antimicrobial activity using the disc-diffusion test.

Microorganisms	Mean Zone of Inhibition (mm $\pm$ SD)		
	CL-Eo (10 $\mu$ L/disc)	Erythromycin (15 $\mu$ g/disc)	Clotrimazole (20 $\mu$ g/disc)
<i>Listeria innocua</i> ATCC 33090	$13.48 \pm 1.65$ <sup>a</sup>	$13.7 \pm 1.56$ <sup>a</sup>	NT
<i>Escherichia coli</i> O157:H7	$12.47 \pm 0.61$ <sup>b</sup>	$10.02 \pm 0.07$ <sup>a</sup>	NT
<i>Proteus mirabilis</i> ATCC 25933	$17.16 \pm 1.04$ <sup>b</sup>	$14.80 \pm 1.73$ <sup>a</sup>	NT
<i>Candida albicans</i> (clinical isolate)	$18.01 \pm 0.91$ <sup>a</sup>	NT	$22.05 \pm 0.73$ <sup>b</sup>
<i>Candida tropicalis</i> (clinical isolate)	$16.45 \pm 0.32$ <sup>a</sup>	NT	$18.23 \pm 0.46$ <sup>b</sup>

SD: standard deviation, NT: not tested. Data sharing the same letter within the same test indicates no significant difference, as determined by Tukey’s multiple range test ( $p < 0.05$ ).

These data highlight the varying sensitivity of different bacterial species to the tested Eo at the indicated doses. It is believed that the antibacterial activity of Eos is attributed to their hydrophobic nature, which is responsible for the destruction of bacterial membranes.

Eos act on bacteria by degrading the cytoplasmic membrane, causing coagulation of the cytoplasm. Additionally, they alter the permeability and function of the membrane [87,88]. However, CL-Eo showed a good antibacterial potential against *P. mirabilis* and a modest level of antibacterial activity against the other bacterial strains. This conclusion is derived from various previous studies that relied on the assumption that the disc-diffusion test, where the assessment of inhibitory zones is as follows: a diameter of 10 mm or less indicates low activity, a diameter between >10 and 15 mm implies moderate activity, and a diameter above 15 mm represents high activity [89,90]. Accordingly, the anti-candidal activity of CL-Eo showed high activity using the disc-diffusion test; *C. albicans* was the most susceptible yeast ( $18.01 \pm 0.91$  mm) followed by *C. tropicalis* ( $16.45 \pm 0.32$  mm) (Table 3). However, for the antibacterial potential, the inhibition zones reported for CL-Eo consistently fell within the range that indicates moderate antibacterial activity for all tested strains except *Protues mirabilis*. The results of the current study are in accordance with Köse et al. [23], who mentioned that the results of the antibacterial properties of *C. ladanifer* hydroalcoholic extract against *E. coli*, *Bacillus subtilis*, and *Enterococcus faecium* recorded moderate activity, with inhibition zones ranging from  $7.56 \pm 0.556$  mm to  $9.59 \pm 0.586$  mm. The findings of this investigation relatively contradict a published study that reported the antibacterial activity of *C. ladanifer* ethanolic and methanolic extracts, with inhibitory zone values ranging from 20 to 23 mm and 20 to 27 mm, respectively. Ferreira et al. [91] stated that through the examination of the outcomes of their disc diffusion experiment, they noticed that the extraction technique used has a substantial impact on the antibacterial activity of *C. ladanifer*.

On the other hand, in this investigation, the MIC assay has been used to ascertain the lowest concentration of the essential oil needed to inhibit microbial growth. The MBC and MFC experiments have also been performed to determine the precise quantity of Eo required to completely eliminate all tested microbes; these results are shown in Table 4. Regarding the tested bacterial strains, the lowest MIC and MBC ratios are recorded for *P. mirabilis* (MIC and MBC = 0.25%), followed by *L. innocua* (MIC = 0.25%, MBC = 0.5%) and *E. coli* (MIC and MBC = 4%). In terms of the tested yeasts, the lowest MIC and MFC ratios are recorded for *C. albicans* (MIC and MBC = 2%), followed by *C. tropicalis* (MIC = 8%, MBC = 16%) (Table 5). The MIC, MBC, and MFC results were in harmony with the disc-diffusion findings and provided further support, emphasizing the need to add these tests in any investigation using plant extracts to improve the accuracy of scientific verification. The MBC/MIC and MFC/MIC ratios indicated bactericidal and fungicidal effects against the tested microorganisms, according to previously established criteria; a plant extract is categorized as bactericidal or fungicidal if the MBC/MIC or MFC/MIC ratios are equal to or less than four, and as bacteriostatic or fungi-static if the MBC/MIC or MFC/MIC ratios exceed four [92].

**Table 4.** MIC and MBC values of CL-Eo.

Bacteria	CL-Eo (% v/v)			Erythromycin (µg/mL)		
	MIC	MBC	MBC/MIC	MIC	MBC	MBC/MIC
<i>L. innocua</i>	0.25	0.5	2	256	256	1
<i>E. coli</i> O157:H7	4	4	1	1024	1024	1
<i>P. mirabilis</i>	0.25	0.25	1	128	1024	4

**Table 5.** MIC, and MFC values of CL-Eo.

Yeasts	CL-Eo (% v/v)			Clotrimazole (µg/mL)		
	MIC	MFC	MFC/MIC	MIC	MFC	MFC/MIC
<i>C. albicans</i>	2	2	1	0.25	0.25	1
<i>C. tropicalis</i>	8	16	2	0.50	0.50	1

Previously published data support the present findings on the efficacy of CL-Eo against *C. albicans* and *C. tropicalis*; Barros et al. [93] cited that the phenolic extract derived from *C. ladanifer* demonstrates a strong reduction in the growth of *C. albicans*, *Candida glabrata*, and *Candida parapsilosis*, with MIC values lower than 0.05 mg/mL. Furthermore, it exhibits a moderate level of inhibition in the growth of *C. tropicalis*, as shown by MIC value of 0.625 mg/mL. It was reported that *C. ladanifer* effectively exhibited low MIC values against *Aspergillus brasiliensis* (MIC = 0.625 mg/mL) and against *Aspergillus fumigatus* (MIC = 5.0 mg/mL) [94]. A published study revealed that *C. ladanifer* has significant antibacterial properties, as reported by MIC and MBC tests conducted on various bacteria, including *S. aureus*, *S. epidermidis*, *P. acnes*, *P. aeruginosa*, *E. coli*, and *K. pneumoniae*. The MIC values varied from 125 to 2000 µg/mL, whereas the MBC values ranged from 1000 to 2000 µg/mL. In addition, *C. ladanifer* had significant anti-candidal activities, as shown by the results of MIC and MFC tests against *C. albicans*. The MIC value was found to be 2000 µg/mL, and the MFC value was higher than 2000 µg/mL [95].

### 3.3.5. Antioxidant Activity

Through the review of the literature, the authors were able to understand the complexities of the oxidation process and the fact that a single technique is not sufficient for providing a thorough assessment of a sample’s antioxidant potential [96]. Consequently, a holistic approach by combining responses obtained from diverse and complementary tests has been opted for. The choice involved employing four chemical tests, specifically assessing the ability of compounds to neutralize free radicals (DPPH, ABTS), inhibit lipid peroxidation (β-carotene bleaching), and evaluate the reducing power of CL-Eo. These tests involved observing visible color changes, which were subsequently analyzed spectrophotometrically at specific wavelengths [97].

In the current study, BHT and α-tocopherol, renowned for their antioxidant properties, were employed as positive controls. The comprehensive results of these tests are presented in Table 6, indicating robust antioxidant activity in scavenging the ABTS•+ radical cation.

**Table 6.** Antioxidant potential of CL-Eo.

Tests/Samples	IC <sub>50</sub> (µg/mL)		
	CL-Eo	BHT	Tocopherol
DPPH	178.29 ± 2.05 <sup>c</sup>	56.11 ± 0.38 <sup>a</sup>	102.45 ± 2.04 <sup>b</sup>
ABTS	134.02 ± 0.67 <sup>c</sup>	74.90 ± 2.56 <sup>b</sup>	48.01 ± 1.17 <sup>a</sup>
FRAP	321.71 ± 4.66 <sup>c</sup>	32.01 ± 1.28 <sup>a</sup>	86.22 ± 4.92 <sup>b</sup>
Beta-carotene	246.14 ± 6.28 <sup>c</sup>	50.4 ± 4.31 <sup>a</sup>	157.6 ± 5.23 <sup>b</sup>

Data sharing the same letter within the same test indicate no significant difference, as determined by Tukey’s multiple range test (*p* < 0.05).

In the test for scavenging activity against the DPPH radical, the evaluation was conducted using a spectrophotometer, tracking the reduction in the DPPH radical, which is characterized by its transition from violet color (DPPH) to yellow color (DPPH-H) measurable at 517 nm [98]. The results revealed that CL-Eo demonstrated a remarkable antioxidant capacity, with IC<sub>50</sub> values of 178.29 ± 2.05 µg/mL. In comparison, the standard antioxidants BHT and α-tocopherol exhibited IC<sub>50</sub> values of 56.11 ± 0.38 and 102.45 ± 2.04 µg/mL, respectively.

In the ABTS<sup>•+</sup> radical scavenger activity test, the method is based on the ability of a substance to neutralize the ABTS<sup>•+</sup> radical in comparison to standard antioxidants (BHT and  $\alpha$ -tocopherol). CL-Eo exhibited an IC<sub>50</sub> value of approximately  $134.02 \pm 0.67$   $\mu\text{g}/\text{mL}$ , while the positive controls demonstrated IC<sub>50</sub> values ranging from  $74.90 \pm 2.56$  to  $48.01 \pm 1.17$   $\mu\text{g}/\text{mL}$  for BHT and  $\alpha$ -tocopherol, respectively.

Concerning the beta-carotene test, the assessment involves the oxidation of linoleic acid, producing peroxide radicals [41]. These radicals consequently oxidize the highly unsaturated  $\beta$ -carotene, resulting in the loss of its orange color [99,100]. The presence of a substance with antioxidant capacity prevents the oxidation and bleaching of  $\beta$ -carotene. The results from this test, as shown in the table, indicate  $\beta$ -carotene whitening activity with an IC<sub>50</sub> of  $246.14 \pm 6.28$   $\mu\text{g}/\text{mL}$ . This value is lower than that of reference drugs BHT and  $\alpha$ -tocopherol, which exhibited IC<sub>50</sub> values of  $50.4 \pm 4.31$  and  $157.6 \pm 5.23$   $\mu\text{g}/\text{mL}$ , respectively.

The reducing capacity of the samples was further investigated by monitoring the transformation of ferric (Fe<sup>3+</sup>) ions into ferrous (Fe<sup>2+</sup>) ions, and the results were determined by measuring absorbance at 700 nm [101]. The results presented in Table 5 highlight the remarkable antioxidant capacity of the studied Eo, with a value of  $321.71 \pm 4.66$   $\mu\text{g}/\text{mL}$ . In comparison, BHT showed an antioxidant capacity of  $32.01 \pm 1.28$   $\mu\text{g}/\text{mL}$ , and  $\alpha$ -tocopherol exhibited a capacity of  $86.22 \pm 4.92$   $\mu\text{g}/\text{mL}$ .

These data surpass those reported by Zidane and colleagues [102], who found that CL-Eo from Eastern Morocco were less effective than the control. To the best of the authors' knowledge and based on the available literature, the assessment of CL-Eo for lipid peroxidation using the  $\beta$ -carotene bleaching assay has not been reported. However, several studies have been conducted to evaluate its antioxidant capacity using DPPH, ABTS, and FRAP techniques. On the other hand, the Eo extracted from the Taza region by Benali et al. [15] exhibited a low anti-DPPH effect with an IC<sub>50</sub> value exceeding 100  $\mu\text{g}/\text{mL}$ . In the FRAP assay, the same authors demonstrated a significant reducing power of ferric ions, with an IC<sub>50</sub> of  $0.1 \pm 0.06$  mg AAE/g of CL-Eo [15].

Sultan Abu-Orabi et al. [103] investigated the antioxidant capacity of volatile oils and crude extracts obtained from the flowers and leaves of *C. salvifolius* and *C. creticus* using various in vitro assays. The leaves Eo of *C. salvifolius* and *C. creticus* demonstrated a higher antiradical potential compared to those derived from the flower parts, with IC<sub>50</sub> values of  $0.16 \pm 0.01$  and  $0.33 \pm 0.01$  mg/mL, respectively, for the DPPH assay. Conversely, the oils from the flowers of *C. salvifolius* and *C. creticus* exhibited a greater antioxidant ability than those obtained from the leaves, with IC<sub>50</sub> values ranging between  $0.09 \pm 0.02$  and  $0.31 \pm 0.01$  mg/mL for the ABTS assay [103]. The antioxidant potential of the Indian CL-Eo was assessed in a study by Neha Upadhyay et al. [104] utilizing DPPH<sup>•</sup> free radical and ABTS<sup>•+</sup> inhibition assays to measure the plant's capacity to quench radicals. CL-Eo exhibited robust radical scavenging action in a dose-dependent manner in both assays. The IC<sub>50</sub> values were determined to be 7.3  $\mu\text{L}/\text{mL}$  for the DPPH<sup>•</sup> assay and 1.13  $\mu\text{L}/\text{mL}$  for the ABTS<sup>•+</sup> test, indicating a significant antioxidant capacity [104].

The potent antioxidant capacities observed in CL-Eo are commonly ascribed to the predominant compounds of Eo, particularly linderol, gamma-terpinene, and borneol, which were revealed as the main components. Generally, the antioxidant ability of volatile oil is a consequence of the synergistic interactions of its plethora of bioactive constituents. Given the significant antioxidant potential of CL-Eo, in vivo investigations are highly recommended to confirm this effect.

#### 4. Conclusions

The current study highlights the chemical characterization and biological efficacy of CL-Eo extracted via microwave-assisted hydrodistillation through in vitro and computational approaches. CL-Eo have shown promising antidiabetic, antimicrobial and antioxidant properties. As evidenced by GC-MS analysis, these properties were generally ascribed to the bioactive compounds revealed in CL-Eo. Indeed, CL-Eo significantly inhibited  $\alpha$ -amylase,  $\alpha$ -glucosidase and lipase enzymes. Moreover, CL-Eo possess effective

antioxidant capacity as indicated by DPPH, ABTS, Frap and beta-carotene tests. CL-Eo demonstrated significant antibacterial activity, especially against *P. mirabilis*. Furthermore, it exhibited effective antifungal activity against *C. albicans* and *C. tropicalis*. The MIC and MBC findings were encouraging and demonstrated their ability to eliminate microorganisms at different levels. In light of these promising results, further investigations should prioritize several crucial areas. Mechanistic studies are needed to examine the molecular basis for the biological properties of CL-Eo. It is essential to conduct in vivo research to assess the effectiveness and safety of this Eo in animal models. Additionally, developing improved formulations suitable for practical uses, such as topical therapies, oral drugs, or disinfectants, is vital. Broadening the scope of examined microorganisms to include a more diverse array of disease-causing bacteria, fungi, and viruses will provide a comprehensive understanding of its antimicrobial potential.

**Author Contributions:** Conceptualization, N.E.H.; methodology, K.F.-B. and F.K.; software A.E.; validation N.E.H.; formal analysis, S.H.A.-M., F.K., K.F.-B., G.N. and E.M.A.; investigation, F.Z.L., M.B., F.K., R.A. and A.E.; resources, N.E.H.; data curation, S.H.A.-M., F.K., K.F.-B., H.N.M. and E.M.A.; writing—original draft preparation, N.E.H., H.N.M., R.A., G.N. and F.K.; writing—review and editing, H.N.M. and K.F.-B.; visualization, N.E.H.; supervision, N.E.H.; project administration, N.E.H.; funding acquisition, N.E.H. All authors have read and agreed to the published version of the manuscript.

**Funding:** This research received no external funding.

**Data Availability Statement:** The original contributions presented in the study are included in the article, further inquiries can be directed to the corresponding author.

**Acknowledgments:** Princess Nourah Bint Abdulrahman University Researchers Supporting Project number (PNURSP2024R158) Princess Nourah Bint Abdulrahman University, Riyadh, Saudi Arabia.

**Conflicts of Interest:** The authors declare no conflicts of interest.

## References

1. Nakanishi, K. A Brief History of Natural Products Chemistry. *Compr. Nat. Prod. Chem.* **1999**, *1*, 8.
2. Abdallah, E.M. Antibacterial Activity of *Hibiscus sabdariffa* L. Calyces against Hospital Isolates of Multidrug Resistant Acinetobacter Baumannii. *J. Acute Dis.* **2016**, *5*, 512–516. [[CrossRef](#)]
3. Petrovska, B.B. Historical Review of Medicinal Plants' Usage. *Pharmacogn. Rev.* **2012**, *6*, 1. [[CrossRef](#)] [[PubMed](#)]
4. Al-Asmari, A.K.; Athar, M.T.; Kadasah, S.G. An Updated Phytopharmacological Review on Medicinal Plant of Arab Region: Apium Graveolens Linn. *Pharmacogn. Rev.* **2017**, *11*, 13. [[CrossRef](#)] [[PubMed](#)]
5. Angane, M.; Swift, S.; Huang, K.; Butts, C.A.; Quek, S.Y. Essential Oils and Their Major Components: An Updated Review on Antimicrobial Activities, Mechanism of Action and Their Potential Application in the Food Industry. *Foods* **2022**, *11*, 464. [[CrossRef](#)]
6. Aprotosoae, A.C.; Gille, E.; Trifan, A.; Luca, V.S.; Miron, A. Essential Oils of Lavandula Genus: A Systematic Review of Their Chemistry. *Phytochem. Rev.* **2017**, *16*, 761–799. [[CrossRef](#)]
7. Chaachouay, N.; Zidane, L. Plant-Derived Natural Products: A Source for Drug Discovery and Development. *Drugs Drug Candidates* **2024**, *3*, 184–207. [[CrossRef](#)]
8. Tortosa, V.; Pietropaolo, V.; Brandi, V.; Macari, G.; Pasquadibisceglie, A.; Polticelli, F. Computational Methods for the Identification of Molecular Targets of Toxic Food Additives. Butylated Hydroxytoluene as a Case Study. *Molecules* **2020**, *25*, 2229. [[CrossRef](#)]
9. Martiz, R.M.; Patil, S.M.; Thirumalapura Hombegowda, D.; Shbeer, A.M.; Alqadi, T.; Al-Ghorbani, M.; Ramu, R.; Prasad, A. Phyto-Computational Intervention of Diabetes Mellitus at Multiple Stages Using Isoeugenol from Ocimum Tenuiflorum: A Combination of Pharmacokinetics and Molecular Modelling Approaches. *Molecules* **2022**, *27*, 6222. [[CrossRef](#)] [[PubMed](#)]
10. Chen, R.; Xu, S.; Ding, Y.; Li, L.; Huang, C.; Bao, M.; Li, S.; Wang, Q. Dissecting Causal Associations of Type 2 Diabetes with 111 Types of Ocular Conditions: A Mendelian Randomization Study. *Front. Endocrinol.* **2023**, *14*, 1307468. [[CrossRef](#)]
11. Khursheed, R.; Singh, S.K.; Wadhwa, S.; Kapoor, B.; Gulati, M.; Kumar, R.; Ramanunni, A.K.; Awasthi, A.; Dua, K. Treatment Strategies against Diabetes: Success so Far and Challenges Ahead. *Eur. J. Pharmacol.* **2019**, *862*, 172625. [[CrossRef](#)] [[PubMed](#)]
12. Ni, Y.-L.; Shen, H.-T.; Chen, S.-P.; Kuan, Y.-H. Protective Effect of Genkwanin against Lipopolysaccharide-Induced Acute Lung Injury in Mice with P38 Mitogen-Activated Protein Kinase and Nuclear Factor- $\kappa$ B Pathway Inhibition. *J. Funct. Foods* **2022**, *98*, 105271. [[CrossRef](#)]
13. Bao, Y.; Sun, Y.-W.; Ji, J.; Gan, L.; Zhang, C.-F.; Wang, C.-Z.; Yuan, C.-S. Genkwanin Ameliorates Adjuvant-Induced Arthritis in Rats through Inhibiting JAK/STAT and NF- $\kappa$ B Signaling Pathways. *Phytomedicine* **2019**, *63*, 153036. [[CrossRef](#)] [[PubMed](#)]

14. Eizirik, D.L.; Pasquali, L.; Cnop, M. Pancreatic  $\beta$ -Cells in Type 1 and Type 2 Diabetes Mellitus: Different Pathways to Failure. *Nat. Rev. Endocrinol.* **2020**, *16*, 349–362. [[CrossRef](#)]
15. Benali, T.; Chtibi, H.; Bouyahya, A.; Khabbach, A.; Hammani, K. Detection of Antioxidant and Antimicrobial Activities in Phenol Components and Essential Oils of *Cistus ladaniferus* and *Mentha suaveolens* Extracts. *Biomed. Pharmacol. J.* **2020**, *13*, 603–612. [[CrossRef](#)]
16. Rădulescu, M.; Jianu, C.; Lukinich-Gruia, A.T.; Mioc, M.; Mioc, A.; Şoica, C.; Stana, L.G. Chemical Composition, in Vitro and in Silico Antioxidant Potential of *Melissa officinalis* Subsp. *officinalis* Essential Oil. *Antioxidants* **2021**, *10*, 1081. [[CrossRef](#)]
17. Bakkali, F.; Averbeck, S.; Averbeck, D.; Idaomar, M. Biological Effects of Essential Oils—A Review. *Food Chem. Toxicol.* **2008**, *46*, 446–475. [[CrossRef](#)]
18. Ashmawy, N.S.; Gad, H.A.; El-Nashar, H.A. Comparative Study of Essential Oils from Different Organs of *Syzygium Cumini* (Pamposia) Based on GC/MS Chemical Profiling and In Vitro Antiaging Activity. *Molecules* **2023**, *28*, 7861. [[CrossRef](#)]
19. Al-Mouhajer, L.; Chabo, R.; Saab, A.M.; Saade, K.; Makhoulouf, H. Antibacterial Activities of Essential Oils Isolated from Two Species *Cupressus arizonica* Greene and *Cupressus sempervirens* L. (var. *horizontalis* and *pyramidalis*). *Eur. J. Biomed. Pharm. Sci* **2017**, *4*, 430–435.
20. Bouyahya, A.; El Omari, N.; Bakha, M.; Aanniz, T.; El Menyiy, N.; El Hachlafi, N.; El Baaboua, A.; El-Shazly, M.; Alshahrani, M.M.; Al Awadh, A.A. Pharmacological Properties of Trichostatin A, Focusing on the Anticancer Potential: A Comprehensive Review. *Pharmaceuticals* **2022**, *15*, 1235. [[CrossRef](#)]
21. Calo, J.R.; Crandall, P.G.; O'Bryan, C.A.; Ricke, S.C. Essential Oils as Antimicrobials in Food Systems—A Review. *Food Control* **2015**, *54*, 111–119.
22. Benali, T.; Bouyahya, A.; Habbadi, K.; Zengin, G.; Khabbach, A.; Achbani, E.H.; Hammani, K. Chemical Composition and Antibacterial Activity of the Essential Oil and Extracts of *Cistus ladaniferus* Subsp. *ladanifer* and *Mentha suaveolens* against Phytopathogenic Bacteria and Their Ecofriendly Management of Phytopathogenic Bacteria. *Biocatal. Agric. Biotechnol.* **2020**, *28*, 101696. [[CrossRef](#)]
23. Köse, M.D.; Tekin, B.N.; Bayraktar, O.; Duman, E.T.; Başpınar, Y. Antioxidant and Antimicrobial Properties of *Cistus ladanifer*. *Int. J. Second. Metab.* **2017**, *4*, 434–444. [[CrossRef](#)]
24. Kosar, M.; Özek, T.; Göger, F.; Kürkcüoğlu, M.; Hüsnü Can Baser, K. Comparison of Microwave-Assisted Hydrodistillation and Hydrodistillation Methods for the Analysis of Volatile Secondary Metabolites. *Pharm. Biol.* **2005**, *43*, 491–495. [[CrossRef](#)]
25. Nouioura, G.; Ghneim, H.K.; Zbadi, L.; Maache, S.; Zouirech, O.; Danouche, M.; Aboul-Soud, M.A.; Giesy, J.P.; Lyoussi, B.; Derwich, E. Exploring the Essence of Celery Seeds (*Apium graveolens* L.): Innovations in Microwave-Assisted Hydrodistillation for Essential Oil Extraction Using In Vitro, In Vivo and In Silico Studies. *Arab. J. Chem.* **2024**, *17*, 105726.
26. Frazão, D.F.; Raimundo, J.R.; Domingues, J.L.; Quintela-Sabaris, C.; Gonçalves, J.C.; Delgado, F. *Cistus ladanifer* (Cistaceae): A Natural Resource in Mediterranean-Type Ecosystems. *Planta* **2018**, *247*, 289–300. [[CrossRef](#)] [[PubMed](#)]
27. Viuda-Martos, M.; Sendra, E.; Pérez-Alvarez, J.A.; Fernández-López, J.; Amensour, M.; Abrini, J. Identification of Flavonoid Content and Chemical Composition of the Essential Oils of Moroccan Herbs: Myrtle (*Myrtus communis* L.), Rockrose (*Cistus ladanifer* L.) and Montpellier Cistus (*Cistus monspeliensis* L.). *J. Essent. Oil Res.* **2011**, *23*, 1–9. [[CrossRef](#)]
28. Taibi, M.; Elbouzidi, A.; Ou-Yahia, D.; Dalli, M.; Bellaouchi, R.; Tikent, A.; Roubi, M.; Gseyra, N.; Asehrou, A.; Hano, C.; et al. Assessment of the Antioxidant and Antimicrobial Potential of *Ptychotis verticillata* Duby Essential Oil from Eastern Morocco: An In Vitro and In Silico Analysis. *Antibiotics* **2023**, *12*, 655. [[CrossRef](#)] [[PubMed](#)]
29. Elbouzidi, A.; Ouassou, H.; Aherkou, M.; Kharchoufa, L.; Meskali, N.; Baraich, A.; Mechchate, H.; Bouhrim, M.; Idir, A.; Hano, C.; et al. LC-MS/MS Phytochemical Profiling, Antioxidant Activity, and Cytotoxicity of the Ethanolic Extract of *Atriplex halimus* L. against Breast Cancer Cell Lines: Computational Studies and Experimental Validation. *Pharmaceuticals* **2022**, *15*, 1156. [[CrossRef](#)]
30. Jianu, C.; Goleţ, I.; Stoin, D.; Cocan, I.; Bujană, G.; Mişcă, C.; Mioc, M.; Mioc, A.; Şoica, C.; Lukinich-Gruia, A.T.; et al. Chemical Profile of *Ruta graveolens*, Evaluation of the Antioxidant and Antibacterial Potential of Its Essential Oil, and Molecular Docking Simulations. *Appl. Sci.* **2021**, *11*, 11753. [[CrossRef](#)]
31. di Giacomo, V.; Recinella, L.; Chiavaroli, A.; Orlando, G.; Cataldi, A.; Rapino, M.; Di Valerio, V.; Politi, M.; Antolini, M.D.; Acquaviva, A.; et al. Metabolomic Profile and Antioxidant/Anti-Inflammatory Effects of Industrial Hemp Water Extract in Fibroblasts, Keratinocytes and Isolated Mouse Skin Specimens. *Antioxidants* **2021**, *10*, 44. [[CrossRef](#)] [[PubMed](#)]
32. El Hachlafi, N.; Fikri-Benbrahim, K.; Al-Mijalli, S.H.; Elbouzidi, A.; Jeddi, M.; Abdallah, E.M.; Assaggaf, H.; Bouyahya, A.; Alnasser, S.M.; Attar, A.; et al. *Tetraclinis articulata* (Vahl) Mast. Essential Oil as a Promising Source of Bioactive Compounds with Antimicrobial, Antioxidant, Anti-Inflammatory and Dermatoprotective Properties: In Vitro and In Silico Evidence. *Heliyon* **2024**, *10*, e23084. [[CrossRef](#)]
33. Fadimu, G.J.; Farahnaky, A.; Gill, H.; Olalere, O.A.; Gan, C.-Y.; Truong, T. In-Silico Analysis and Antidiabetic Effect of  $\alpha$ -Amylase and  $\alpha$ -Glucosidase Inhibitory Peptides from Lupin Protein Hydrolysate: Enzyme-Peptide Interaction Study Using Molecular Docking Approach. *Foods* **2022**, *11*, 3375. [[CrossRef](#)] [[PubMed](#)]
34. Etsassala, N.G.E.R.; Badmus, J.A.; Marnewick, J.L.; Egieyeh, S.; Iwuoha, E.I.; Nchu, F.; Hussein, A.A. Alpha-Glucosidase and Alpha-Amylase Inhibitory Activities, Molecular Docking, and Antioxidant Capacities of *Plectranthus Ecklonii* Constituents. *Antioxidants* **2022**, *11*, 378. [[CrossRef](#)] [[PubMed](#)]
35. Nguyen, P.T.; Huynh, H.A.; Truong, D.V.; Tran, T.-D.; Vo, C.-V.T. Exploring Aurone Derivatives as Potential Human Pancreatic Lipase Inhibitors through Molecular Docking and Molecular Dynamics Simulations. *Molecules* **2020**, *25*, 4657. [[CrossRef](#)] [[PubMed](#)]

36. Al-Mijalli, S.H.; Mrabti, H.N.; El Hachlafi, N.; El Kamili, T.; Elbouzidi, A.; Abdallah, E.M.; Flouchi, R.; Assaggaf, H.; Qasem, A.; Zengin, G. Integrated Analysis of Antimicrobial, Antioxidant, and Phytochemical Properties of Cinnamomum Verum: A Comprehensive In Vitro and In Silico Study. *Biochem. Syst. Ecol.* **2023**, *110*, 104700. [[CrossRef](#)]
37. Thalapaneni, N.R.; Chidambaram, K.A.; Ellappan, T.; Sabapathi, M.L.; Mandal, S.C. Inhibition of Carbohydrate Digestive Enzymes by *Talinum portulacifolium* (Forssk) Leaf Extract. *J. Complement. Integr. Med.* **2008**, *5*, 6–16. [[CrossRef](#)]
38. Sugiwati, S.; Setiasih, S.; Afifah, E. Antihyperglycemic Activity of the Mahkota Dewa Leaf Extracts as an Alpha-Glucosidase Inhibitor. *Makara J. Health Res.* **2009**, *13*, 74–78. [[CrossRef](#)]
39. McDougall, G.J.; Kulkarni, N.N.; Stewart, D. Berry Polyphenols Inhibit Pancreatic Lipase Activity In Vitro. *Food Chem.* **2009**, *115*, 193–199. [[CrossRef](#)]
40. Vinson, J.A.; Howard III, T.B. Inhibition of Protein Glycation and Advanced Glycation End Products by Ascorbic Acid and Other Vitamins and Nutrients. *J. Nutr. Biochem.* **1996**, *7*, 659–663. [[CrossRef](#)]
41. El Hachlafi, N.; Mrabti, H.N.; Al-Mijalli, S.H.; Jeddi, M.; Abdallah, E.M.; Benkhaira, N.; Hadni, H.; Assaggaf, H.; Qasem, A.; Goh, K.W.; et al. Antioxidant, Volatile Compounds; Antimicrobial, Anti-Inflammatory, and Dermatoprotective Properties of Cedrus Atlantica (Endl.) Manetti Ex Carriere Essential Oil: In Vitro and In Silico Investigations. *Molecules* **2023**, *28*, 5913. [[CrossRef](#)] [[PubMed](#)]
42. Hombach, M.; Bloemberg, G.V.; Böttger, E.C. Effects of Clinical Breakpoint Changes in CLSI Guidelines 2010/2011 and EUCAST Guidelines 2011 on Antibiotic Susceptibility Test Reporting of Gram-Negative Bacilli. *J. Antimicrob. Chemother.* **2012**, *67*, 622–632. [[CrossRef](#)] [[PubMed](#)]
43. Mrabti, H.N.; El Hachlafi, N.; Al-Mijalli, S.H.; Jeddi, M.; Elbouzidi, A.; Abdallah, E.M.; Flouchi, R.; Assaggaf, H.; Qasem, A.; Zengin, G. Phytochemical Profile, Assessment of Antimicrobial and Antioxidant Properties of Essential Oils of Artemisia Herba-Alba Asso., and Artemisia Dracunculus L.: Experimental and Computational Approaches. *J. Mol. Struct.* **2023**, *1294*, 136479. [[CrossRef](#)]
44. Jaradat, N.; Al-Maharik, N.; Abdallah, S.; Shawahna, R.; Mousa, A.; Qtishat, A. Nepeta Curviflora Essential Oil: Phytochemical Composition, Antioxidant, Anti-Proliferative and Anti-Migratory Efficacy against Cervical Cancer Cells, and  $\alpha$ -Glucosidase,  $\alpha$ -Amylase and Porcine Pancreatic Lipase Inhibitory Activities. *Ind. Crops Prod.* **2020**, *158*, 112946. [[CrossRef](#)]
45. Villaño, D.; Fernández-Pachón, M.S.; Moyá, M.L.; Troncoso, A.M.; García-Parrilla, M.C. Radical Scavenging Ability of Polyphenolic Compounds towards DPPH Free Radical. *Talanta* **2007**, *71*, 230–235. [[CrossRef](#)] [[PubMed](#)]
46. El Omari, N.; Sayah, K.; Fettach, S.; El Blidi, O.; Bouyahya, A.; Faouzi, M.E.A.; Kamal, R.; Barkiyou, M. Evaluation of in Vitro Antioxidant and Antidiabetic Activities of Aristolochia Longa Extracts. *Evid.-Based Complement. Altern. Med.* **2019**, *2019*, 7384735. [[CrossRef](#)]
47. Benzie, I.F.; Strain, J.J. The Ferric Reducing Ability of Plasma (FRAP) as a Measure of “Antioxidant Power”: The FRAP Assay. *Anal. Biochem.* **1996**, *239*, 70–76. [[CrossRef](#)]
48. Gulluce, M.; Sahin, F.; Sokmen, M.; Ozer, H.; Daferera, D.; Sokmen, A.; Polissiou, M.; Adiguzel, A.; Ozkan, H. Antimicrobial and Antioxidant Properties of the Essential Oils and Methanol Extract from *Mentha longifolia* L. Ssp. Longifolia. *Food Chem.* **2007**, *103*, 1449–1456. [[CrossRef](#)]
49. Greche, H.; Mrabet, N.; Zrira, S.; Ismaili-Alaoui, M.; Benjlali, B.; Boukir, A. The Volatiles of the Leaf Oil of *Cistus ladanifer* L. Var. *albiflorus* and Labdanum Extracts of Moroccan Origin and Their Antimicrobial Activities. *J. Essent. Oil Res.* **2009**, *21*, 166–173. [[CrossRef](#)]
50. Sharifi-Rad, M.; Varoni, E.M.; Iriti, M.; Martorell, M.; Setzer, W.N.; Del Mar Contreras, M.; Salehi, B.; Soltani-Nejad, A.; Rajabi, S.; Tajbakhsh, M.; et al. Carvacrol and Human Health: A Comprehensive Review. *Phytother. Res.* **2018**, *32*, 1675–1687. [[CrossRef](#)]
51. Al-Farhan, K.; Warad, I.; Al-Resayes, S.; Fouda, M.; Ghazzali, M. Synthesis, Structural Chemistry and Antimicrobial Activity of  $\alpha$ -Borneol Derivative. *Open Chem.* **2010**, *8*, 1127–1133. [[CrossRef](#)]
52. Ramalho, T.; Pacheco De Oliveira, M.; Lima, A.; Bezerra-Santos, C.; Piuvezam, M. Gamma-Terpinene Modulates Acute Inflammatory Response in Mice. *Planta Med.* **2015**, *81*, 1248–1254. [[CrossRef](#)] [[PubMed](#)]
53. Hachlafi, N.E.; Aanniz, T.; Menyiy, N.E.; Baaboua, A.E.; Omari, N.E.; Balahbib, A.; Shariati, M.A.; Zengin, G.; Fikri-Benbrahim, K.; Bouyahya, A. In Vitro and In Vivo Biological Investigations of Camphene and Its Mechanism Insights: A Review. *Food Rev. Int.* **2023**, *39*, 1799–1826. [[CrossRef](#)]
54. El Karkouri, J.; Bouhrim, M.; Al Kamaly, O.M.; Mechchate, H.; Kchibale, A.; Adadi, I.; Amine, S.; Alaoui Ismaili, S.; Zair, T. Chemical Composition, Antibacterial and Antifungal Activity of the Essential Oil from *Cistus ladanifer* L. *Plants* **2021**, *10*, 2068. [[CrossRef](#)] [[PubMed](#)]
55. Pérez-Izquierdo, C.; Jordán Bueso, M.J.; Rodríguez-Molina, M.d.C.; Pulido, F. Spatial Variation in Yield, Chemical Composition, and Phytotoxic Activity of *Cistus ladanifer* Essential Oils. *Chem. Biodivers.* **2023**, *20*, e202300995. [[CrossRef](#)]
56. Verdeguer, M.; Blázquez, M.A.; Boira, H. Chemical Composition and Herbicidal Activity of the Essential Oil from a *Cistus ladanifer* L. Population from Spain. *Nat. Prod. Res.* **2012**, *26*, 1602–1609. [[CrossRef](#)] [[PubMed](#)]
57. Jeddi, M.; El Hachlafi, N.; El Fadili, M.; Benkhaira, N.; Al-Mijalli, S.H.; Kandsi, F.; Abdallah, E.M.; Ouaritini, Z.B.; Bouyahya, A.; Lee, L.-H. Antimicrobial, Antioxidant,  $\alpha$ -Amylase and  $\alpha$ -Glucosidase Inhibitory Activities of a Chemically Characterized Essential Oil from *Lavandula angustifolia* Mill.: In Vitro and In Silico Investigations. *Biochem. Syst. Ecol.* **2023**, *111*, 104731. [[CrossRef](#)]

58. Gomes, P.B.; Mata, V.G.; Rodrigues, A.E. Characterization of the Portuguese-Grown *Cistus ladanifer* Essential Oil. *J. Essent. Oil Res.* **2005**, *17*, 160–165. [[CrossRef](#)]
59. Pinzi, L.; Rastelli, G. Molecular Docking: Shifting Paradigms in Drug Discovery. *Int. J. Mol. Sci.* **2019**, *20*, 4331. [[CrossRef](#)]
60. Adelusi, T.I.; Oyedele, A.-Q.K.; Boyenle, I.D.; Ogunlana, A.T.; Adeyemi, R.O.; Ukachi, C.D.; Idris, M.O.; Olaoba, O.T.; Adedotun, I.O.; Kolawole, O.E. Molecular Modeling in Drug Discovery. *Inform. Med. Unlocked* **2022**, *29*, 100880. [[CrossRef](#)]
61. Abdanipour, A.; Nejatbakhsh, R.; Jafari Anarkooli, I.; Ghorbanlo, M.; Nikfar, A.; Noriyan, A. Proliferation and Anti-Apoptotic Effect of Hydroethanolic Extract of *Lavandula Officinalis* on Rat Neural Stem Cells. *J. Adv. Med. Biomed. Res.* **2016**, *24*, 43–52.
62. Baysal, T.; Demirdöven, A. Lipoxygenase in Fruits and Vegetables: A Review. *Enzym. Microb. Technol.* **2007**, *40*, 491–496. [[CrossRef](#)]
63. Brash, A.R. Lipoxygenases: Occurrence, Functions, Catalysis, and Acquisition of Substrate. *J. Biol. Chem.* **1999**, *274*, 23679–23682. [[CrossRef](#)]
64. Haeggström, J.Z. Leukotriene Biosynthetic Enzymes as Therapeutic Targets. *J. Clin. Investig.* **2018**, *128*, 2680–2690. [[CrossRef](#)]
65. Attjioui, M.; Ryan, S.; Ristic, A.K.; Higgins, T.; Gofni, O.; Gibney, E.R.; Tierney, J.; O’Connell, S. Comparison of Edible Brown Algae Extracts for the Inhibition of Intestinal Carbohydrate Digestive Enzymes Involved in Glucose Release from the Diet. *J. Nutr. Sci.* **2021**, *10*, e5. [[CrossRef](#)]
66. Qurtam, A.A.; Mechchate, H.; Es-safi, I.; Al-zharani, M.; Nasr, F.A.; Noman, O.M.; Aleissa, M.; Imtara, H.; Aleissa, A.M.; Bouhrim, M.; et al. Citrus Flavanone Narirutin, In Vitro and In Silico Mechanistic Antidiabetic Potential. *Pharmaceutics* **2021**, *13*, 1818. [[CrossRef](#)]
67. Mechchate, H.; Es-Safi, I.; Bourhia, M.; Kyrylchuk, A.; El Moussaoui, A.; Conte, R.; Ullah, R.; Ezzeldin, E.; Mostafa, G.A.; Grafov, A.; et al. In-Vivo Antidiabetic Activity and In-Silico Mode of Action of LC/MS-MS Identified Flavonoids in Oleaster Leaves. *Molecules* **2020**, *25*, 5073. [[CrossRef](#)]
68. Suvd, D.; Fujimoto, Z.; Takase, K.; Matsumura, M.; Mizuno, H. Crystal Structure of *Bacillus Stearothermophilus*  $\alpha$ -Amylase: Possible Factors Determining the Thermostability. *J. Biochem.* **2001**, *129*, 461–468. [[CrossRef](#)] [[PubMed](#)]
69. Aghajari, N.; Haser, R.; Feller, G.; Gerday, C. Crystal Structures of the Psychrophilic  $\alpha$ -Amylase from *Alteromonas Haloplanctis* in Its Native Form and Complexed with an Inhibitor. *Protein Sci.* **1998**, *7*, 564–572. [[CrossRef](#)] [[PubMed](#)]
70. Rangunath, C.; Manuel, S.G.A.; Kasinathan, C.; Ramasubbu, N. Structure-Function Relationships in Human Salivary  $\alpha$ -Amylase: Role of Aromatic Residues in a Secondary Binding Site. *Biologia* **2008**, *63*, 1028–1034. [[CrossRef](#)]
71. Rangunath, C.; Manuel, S.G.A.; Venkataraman, V.; Sait, H.B.R.; Kasinathan, C.; Ramasubbu, N. Probing the Role of Aromatic Residues at the Secondary Saccharide-Binding Sites of Human Salivary  $\alpha$ -Amylase in Substrate Hydrolysis and Bacterial Binding. *J. Mol. Biol.* **2008**, *384*, 1232–1248. [[CrossRef](#)]
72. Liu, T.-T.; Liu, X.-T.; Chen, Q.-X.; Shi, Y. Lipase Inhibitors for Obesity: A Review. *Biomed. Pharmacother.* **2020**, *128*, 110314. [[CrossRef](#)]
73. İnan, Y.; Akyüz, S.; Kurt-Celep, I.; Celep, E.; Yesilada, E. Influence of in Vitro Human Digestion Simulation on the Phenolics Contents and Biological Activities of the Aqueous Extracts from Turkish *Cistus* Species. *Molecules* **2021**, *26*, 5322. [[CrossRef](#)] [[PubMed](#)]
74. Sayah, K.; Marmouzi, I.; Naceiri Mrabti, H.; Cherrah, Y.; Faouzi, M.E.A. Antioxidant Activity and Inhibitory Potential of *Cistus salviifolius* (L.) and *Cistus Monspeliensis* (L.) Aerial Parts Extracts against Key Enzymes Linked to Hyperglycemia. *BioMed Res. Int.* **2017**, *2017*, 2789482. [[CrossRef](#)]
75. Hitl, M.; Bijelić, K.; Stilinović, N.; Božin, B.; Srđenović-Čonić, B.; Torović, L.; Kladar, N. Phytochemistry and Antihyperglycemic Potential of *Cistus salviifolius* L., Cistaceae. *Molecules* **2022**, *27*, 8003. [[CrossRef](#)] [[PubMed](#)]
76. Tan, X.C.; Chua, K.H.; Ravishankar Ram, M.; Kuppusamy, U.R. Monoterpenes: Novel Insights into Their Biological Effects and Roles on Glucose Uptake and Lipid Metabolism in 3T3-L1 Adipocytes. *Food Chem.* **2016**, *196*, 242–250. [[CrossRef](#)] [[PubMed](#)]
77. Kochar Kaur, K.; Allahbadia, G.; Singh, M. Monoterpenes—A Class of Terpenoid Group of Natural Products as a Source of Natural Antidiabetic Agents in the Future—A Review. *CPQ Nutr.* **2019**, *3*, 1–21.
78. Kaur, G.; Tharappel, L.J.P.; Kumawat, V. Evaluation of Safety and in Vitro Mechanisms of Anti-Diabetic Activity of  $\beta$ -Caryophyllene and L-Arginine. *J. Biol. Sci.* **2018**, *18*, 124–134. [[CrossRef](#)]
79. Aazza, S.; El-Guendouz, S.; Miguel, M.G.; Dulce Antunes, M.; Leonor Faleiro, M.; Isabel Correia, A.; Cristina Figueiredo, A. Antioxidant, Anti-Inflammatory and Anti-Hyperglycaemic Activities of Essential Oils from *Thymbra Capitata*, *Thymus Albicans*, *Thymus Caespititius*, *Thymus Carnosus*, *Thymus Lotocephalus* and *Thymus Mastichina* from Portugal. *Nat. Prod. Commun.* **2016**, *11*, 1029–1038. [[CrossRef](#)]
80. Mehdzadeh, L.; Moghaddam, M. Chapter 10—Essential Oils: Biological Activity and Therapeutic Potential. In *Holban Probiotic, and Unconventional Foods*; Academic Press: Cambridge, MA, USA, 2018; pp. 167–179. ISBN 978-0-12-814625-5.
81. Fruh, S.M. Obesity: Risk Factors, Complications, and Strategies for Sustainable Long-term Weight Management. *J. Am. Assoc. Nurse Pract.* **2017**, *29*, S3–S14. [[CrossRef](#)] [[PubMed](#)]
82. Aji, O.R.; Hudaya, R.A.; Putri, D.A. In Vitro Pancreatic Lipase Inhibitor Activity of *Mangifera Foetida* Leaves Extract. *Biodjati* **2021**, *6*, 82–92. [[CrossRef](#)]



83. Benrahou, K.; Naceiri Mrabti, H.; Bouyahya, A.; Daoudi, N.E.; Bnouham, M.; Mezzour, H.; Mahmud, S.; Alshahrani, M.M.; Obaidullah, A.J.; Cherrah, Y.; et al. Inhibition of  $\alpha$ -Amylase,  $\alpha$ -Glucosidase, and Lipase, Intestinal Glucose Absorption, and Antidiabetic Properties by Extracts of *Erodium Guttatum*. *Evid.-Based Complement. Altern. Med.* **2022**, *2022*, 5868682. [[CrossRef](#)] [[PubMed](#)]
84. Vlassopoulos, A.; Mikrou, T.; Papantoni, A.; Papadopoulos, G.; Kapsokefalou, M.; Mallouchos, A.; Gardeli, C. The Effect of Terpenoid Compounds on the Formation of Advanced Glycation Endproducts (AGEs) in Model Systems. *Appl. Sci.* **2022**, *12*, 908. [[CrossRef](#)]
85. Asgary, S.; Naderi, G.A.; Sahebkar, A.; Ardekani, M.R.S.; Kasher, T.; Aslani, S.; Airin, A.; Emami, S.A. Essential Oils from the Fruits and Leaves of *Juniperus Sabina* Possess Inhibitory Activity against Protein Glycation and Oxidative Stress: An In Vitro Phytochemical Investigation. *J. Essent. Oil Res.* **2013**, *25*, 70–77. [[CrossRef](#)]
86. Bernacka, K.; Bednarska, K.; Starzec, A.; Mazurek, S.; Fecka, I. Antioxidant and Antiglycation Effects of *Cistus × Incanus* Water Infusion, Its Phenolic Components, and Respective Metabolites. *Molecules* **2022**, *27*, 2432. [[CrossRef](#)] [[PubMed](#)]
87. Man, A.; Santacroce, L.; Iacob, R.; Mare, A.; Man, L. Antimicrobial Activity of Six Essential Oils against a Group of Human Pathogens: A Comparative Study. *Pathogens* **2019**, *8*, 15. [[CrossRef](#)] [[PubMed](#)]
88. Nazzaro, F.; Fratianni, F.; De Martino, L.; Coppola, R.; De Feo, V. Effect of Essential Oils on Pathogenic Bacteria. *Pharmaceuticals* **2013**, *6*, 1451–1474. [[CrossRef](#)]
89. AlRajhi, M.; Al-Rasheedi, M.; Eltom, S.E.M.; Alhazmi, Y.; Mustafa, M.M.; Ali, A.M. Antibacterial Activity of Date Palm Cake Extracts (*Phoenix Dactylifera*). *Cogent Food Agric.* **2019**, *5*, 1625479. [[CrossRef](#)]
90. Ji, Y.; Hu, W.; Guan, Y.; Saren, G. Effects of Plant Essential Oil Treatment on the Growth of Pathogenic Fungi and the Activity of Defense-Related Enzymes of Fungi-Inoculated Blueberry. *Horticulturae* **2024**, *10*, 318. [[CrossRef](#)]
91. Ferreira, S.; Santos, J.; Duarte, A.; Duarte, A.P.; Queiroz, J.A.; Domingues, F.C. Screening of Antimicrobial Activity of *Cistus ladanifer* and *Arbutus unedo* Extracts. *Nat. Prod. Res.* **2012**, *26*, 1558–1560. [[CrossRef](#)] [[PubMed](#)]
92. Davis, J.L. Pharmacologic Principles. *Equine Intern. Med.* **2018**, *4*, 79–137.
93. Barros, L.; Duenas, M.; Alves, C.T.; Silva, S.; Henriques, M.; Santos-Buelga, C.; Ferreira, I.C. Antifungal Activity and Detailed Chemical Characterization of *Cistus ladanifer* Phenolic Extracts. *Ind. Crops Prod.* **2013**, *41*, 41–45. [[CrossRef](#)]
94. Rihab, G. Valorisation of *Cistus ladanifer* L. Biomass as a Source of Compounds for Bio-Based Industries. Ph.D. Thesis, Polytechnic Institute of Bragança, Bragança, Portugal, 2022.
95. Bouabidi, M.; Salamone, F.L.; Gadhi, C.; Bouamama, H.; Speciale, A.; Ginestra, G.; Pulvirenti, L.; Siracusa, L.; Nostro, A.; Cristani, M. Efficacy of Two Moroccan *Cistus* Species Extracts against *Acne Vulgaris*: Phytochemical Profile, Antioxidant, Anti-Inflammatory and Antimicrobial Activities. *Molecules* **2023**, *28*, 2797. [[CrossRef](#)] [[PubMed](#)]
96. Padmanabhan, P.; Jangle, S.N. Evaluation of DPPH Radical Scavenging Activity and Reducing Power of Four Selected Medicinal Plants and Their Combinations. *Int. J. Pharm. Sci. Drug Res.* **2012**, *4*, 143–146.
97. Nouioura, G.; Tourabi, M.; El Ghouizi, A.; Kara, M.; Assouguem, A.; Saleh, A.; Kamaly, O.A.; El Ouadrhiri, F.; Lyoussi, B.; Derwich, E.H. Optimization of a New Antioxidant Formulation Using a Simplex Lattice Mixture Design of *Apium Graveolens* L., *Coriandrum Sativum* L., and *Petroselinum Crispum* M. Grown in Northern Morocco. *Plants* **2023**, *12*, 1175. [[CrossRef](#)] [[PubMed](#)]
98. De Menezes, B.B.; Frescura, L.M.; Duarte, R.; Villetti, M.A.; Da Rosa, M.B. A Critical Examination of the DPPH Method: Mistakes and Inconsistencies in Stoichiometry and IC50 Determination by UV-Vis Spectroscopy. *Anal. Chim. Acta* **2021**, *1157*, 338398. [[CrossRef](#)] [[PubMed](#)]
99. Yeo, J.; Shahidi, F. Revisiting DPPH (2,2-Diphenyl-1-Picrylhydrazyl) Assay as a Useful Tool in Antioxidant Evaluation: A New IC100 Concept to Address Its Limitations. *J. Food Bioact.* **2019**, *7*, 36–42. [[CrossRef](#)]
100. Miguel, M.G. Antioxidant and Anti-Inflammatory Activities of Essential Oils: A Short Review. *Molecules* **2010**, *15*, 9252–9287. [[CrossRef](#)]
101. Platzer, M.; Kiese, S.; Tybussek, T.; Herfellner, T.; Schneider, F.; Schweiggert-Weisz, U.; Eisner, P. Radical Scavenging Mechanisms of Phenolic Compounds: A Quantitative Structure-Property Relationship (QSPR) Study. *Front. Nutr.* **2022**, *9*, 882458. [[CrossRef](#)]
102. Zidane, H.; Elmiz, M.; Aouinti, F.; Tahani, A.; Wathelet, J.; Sindic, M.; Elbachiri, A. Chemical Composition and Antioxidant Activity of Essential Oil, Various Organic Extracts of *Cistus ladanifer* and *Cistus Libanotis* Growing in Eastern Morocco. *Afr. J. Biotechnol.* **2013**, *12*, 5314–5320. [[CrossRef](#)]
103. Abu-Orabi, S.T.; Al-Qudah, M.A.; Saleh, N.R.; Bataineh, T.T.; Obeidat, S.M.; Al-Sheraideh, M.S.; Al-Jaber, H.I.; Tashtoush, H.I.; Lahham, J.N. Antioxidant Activity of Crude Extracts and Essential Oils from Flower Buds and Leaves of *Cistus Creticus* and *Cistus salviifolius*. *Arab. J. Chem.* **2020**, *13*, 6256–6266. [[CrossRef](#)]
104. Upadhyay, N.; Singh, V.K.; Dwivedy, A.K.; Das, S.; Chaudhari, A.K.; Dubey, N.K. *Cistus ladanifer* L. Essential Oil as a Plant Based Preservative against Molds Infesting Oil Seeds, Aflatoxin B1 Secretion, Oxidative Deterioration and Methylglyoxal Biosynthesis. *LWT* **2018**, *92*, 395–403. [[CrossRef](#)]

**Disclaimer/Publisher’s Note:** The statements, opinions and data contained in all publications are solely those of the individual author(s) and contributor(s) and not of MDPI and/or the editor(s). MDPI and/or the editor(s) disclaim responsibility for any injury to people or property resulting from any ideas, methods, instructions or products referred to in the content.